Estimating occupancy for Montana bat species prior to the arrival of white-nose syndrome

Wilson J. Wright[1], Andrea R. Litt[1], and Emily S. Almberg[2]

[1] Montana State University, Department of Ecology,
Bozeman, MT 59717

[2] Montana Fish, Wildlife, and Parks,
Bozeman, MT 59718

[*]E-mail: wilson.wright@msu.montana.edu

Disclaimer: This manuscript has not gone through a formal review process. This work is in partial fulfillment of Agreement 18-519 between Montana State University and Montana Fish, Wildlife, and Parks.

Summary

The spread of white-nose syndrome (WNS) across the eastern United States has raised conservation concerns and provided motivation for efforts to monitor the impacts of this disease. Currently, WNS has not yet been detected in Montana, or any other western state besides Washington, and it is unknown how severe it will impact species in this region once it arrives. Within an occupancy model framework, we analyzed mist netting and acoustic records for eight bat species in Montana to estimate baseline distributions across the state prior to the arrival of WNS. Heterogeneity in the probabilities of occupancy for each species was explained with covariates for forest cover (%), elevation, ruggedness, and average degree days. Our analysis provided no evidence of spatial correlation among occupancy probabilities within each species, but did suggest spatial correlation among detection probabilities likely related to timing of surveys. We incorporated spatially-correlated random effects in the model for detection probabilities to account for these patterns. The species distribution maps resulting from this analysis can be compared to future distribution maps, after the arrival of WNS, to better understand impacts of the disease in the state. Estimates from this model can also provide guidance for future bat monitoring within the state by helping to focus surveillance efforts on areas with high predicted probabilities of occupancy or optimizing surveys to reduce uncertainty in subsequent analyses.

Introduction

Wildlife management and conservation efforts often rely on mapping species distributions and assessing how they are impacted by various factors. These factors can include management actions, disease, and changing environments, which all have potential to drastically change where wildlife populations occur. Many North American bat populations are currently facing massive population declines (Frick, Pollock, et al. 2010; Langwig, Frick, Bried, et al. 2012) due to the spread of white-nose syndrome (WNS), which could lead to geographically-extensive distribution changes. Recent bat conservation efforts to understand and monitor the impacts of this disease exemplify the importance of assessing species dis-

tributions over time. Bat populations in the eastern United States have been decimated by WNS, including one previously common species (Frick, Pollock, et al. 2010), and this disease has been steadily spreading westward (Frick, Puechmaille, & Willis 2016). Currently, however, WNS has not yet been detected in Montana, or any other western state besides Washington, and it is unknown whether the impacts of the disease in this region will be as extreme as those in eastern states. In addition to differing by bat species, mortality rates of WNS are related to roost environmental conditions and social group size (Langwig, Frick, Bried, et al. 2012), both of which are different in Montana compared to the roosts typically found in eastern states. Understanding how WNS impacts bat populations in western states requires accurate assessments of current species distributions and continued monitoring after the disease arrives. To inform baseline bat distributions within Montana and help guide future monitoring efforts, we analyzed existing data to map the distributions of eight bat species within the state.

We used an occupancy modeling framework to analyze data and estimate species distributions. While there are many different types of species distribution models, occupancy models have been shown to be an effective tool for assessing and monitoring bat populations over large regions (Rodhouse, Ormsbee, Irvine, & Vierlin 2012; Rodhouse, Ormsbee, Irvine, Vierling, et al. 2015). Occupancy models use multiple visits to designated sites to simultaneously estimate both the probability of detecting a species and the probability it is present at a site (MacKenzie, Nichols, et al. 2002). Generally, other types of species distribution models fail to explicitly account for imperfect detection and, consequently, any estimates of the underlying ecological process of interest are confounded with detection (Yackulic et al. 2013; Kéry & Royle 2016, pages 554-557). This makes interpretation of estimates difficult because it is impossible to distinguish whether any apparent patterns are a result of differences in detection, occupancy, or both. Occupancy models, on the other hand, can be used to avoid this issue by directly estimating occurrence probabilities while still accounting for imperfect detection. Bats are notoriously difficult to survey and often have low detection

probabilities (e.g.; Rodhouse, Ormsbee, Irvine, & Vierlin 2012; Rodhouse, Ormsbee, Irvine, Vierling, et al. 2015), emphasizing the importance of modeling detection when estimating occupancy. Better understanding of the detection process itself is also beneficial for planning future surveys with the goal of reducing uncertainty in any subsequent analyses.

To estimate occupancy, we analyzed detection/non-detection data for eight bat species available from mist netting and acoustic monitoring across Montana during the summers of 2008, 2009, and 2010. While additional years are available for these data, we used this subset because it focuses on a relatively short time span which is more aligned with the assumptions of occupancy models. Additionally, these years provide the most observations and have good geographic coverage across the entire state. More recent acoustic monitoring data available in Montana are not as well-suited for estimating occupancy because of the limited geographic coverage, visits spanning longer time periods, and uncertainty regarding species identifications for many records. These additional data may be useful for estimating baseline bat activity patterns as they relate to covariates, assessing year-round activity levels, and understanding the acoustic detection process for bats in more detail all prior to the arrival of WNS. We will focus on these more recent bat acoustic data in future analyses. Other sources of data, such as WNS surveillance efforts and microclimate information from known hibernacula, will also be crucial for understanding the impacts of WNS in Montana. While estimating baseline species distributions for the state is an important piece of information, it is just one of many steps to better assess and monitor how WNS affects bat populations in the state.

Methods

Data

Mist netting and acoustic data were collected by Montana Fish, Wildlife, and Parks and their partners then housed by the Montana Natural Heritage Program. These data include records from 1989 to 2016 for the mist net captures and from 2003 to 2012 for the

acoustic detections. The acoustic detections we used in this analysis are from Pettersson detectors deployed across the state with each deployment being over a relatively short time span. Additional bat acoustic records are available for Montana across a network of long-term deployments where each detector was typically stationed at a single location for longer than a year. These long-term deployments are not analyzed here but will be the focus of future analyses that focus on baseline bat activity patterns. The entire dataset includes some observations from outside of Montana but we only include observations from Montana in the analysis.

From the entire dataset, the acoustic records include 13 different bat species: Townsend's big-eared (*Corynorhinus townsendii*; COTO), big brown (*Eptesicus fuscus*; EPFU), spotted (*Euderma maculatum*; EUMA), silver-haired (*Lasionycteris noctivagans*; LANO), eastern red (*Lasiurus borealis*; LABO), hoary (*Lasiurus cinereus*; LACI), California Myotis (*Myotis californicus*; MYCA), western small-footed Myotis (*Myotis ciliolabrum*; MYCI), long-eared Myotis (*Myotis evotis*; MYEV), little brown Myotis (*Myotis lucifugus*; MYLU), fringed Myotis (*Myotis thysanodes*; MYTH), long-legged Myotis (*Myotis volans*; MYVO), and yuma Myotis (*Myotis yumanensis*; MYYU). The mist netting records include all of these species as well as the pallid bat (*Antrozous pallidus*; ANPA) and northern Myotis (*Myotis septentrionalis*; MYSE). For the remainder of this report we refer to each species using four letter species codes created by combining the first two letters of the genus with the first two letters of the species epithet (e.g., big brown bat, *Eptesicus fuscus*, referred to as EPFU), as noted above.

We used observations collected during the summers (defined as June-September) of 2008, 2009, and 2010 to estimate species distributions. As mentioned previously, these years were selected because they provided good geographic coverage across the state and the greatest effort in terms of total nights sampled. Each record includes the date sampled, geographic coordinates for the location, and indicators for whether each species was detected/captured (1) or not (0) for that particular night. We assume there are no false positive detections in

these data and that all detections/captures unequivocally indicate presence of the species at that location. Our analysis focused on eight of the available species: EPFU, LANO, LACI, MYCA, MYCI, MYEV, MYLU, and MYVO. We determined there were too few detections to estimate occupancy for the remaining species.

Of the bat species included in our analysis, EPFU and MYLU are known to be susceptible to WNS (Langwig, Frick, Reynolds, et al. 2015; Frick, Puechmaille, & Willis 2016). The fungus causing WNS has also been detected on LANO, but individuals have not shown symptoms of the actual disease (Bernard et al. 2015). Additionally, WNS affects many other species in the *Myotis* genus in both North America (Langwig, Frick, Reynolds, et al. 2015; Frick, Puechmaille, & Willis 2016) and Europe (but without the high mortality rate; Wibbelt et al. 2010). Most of the other species included in our analysis are suspected to be susceptible because of their close relatedness to species known to be affected by WNS (i.e.,

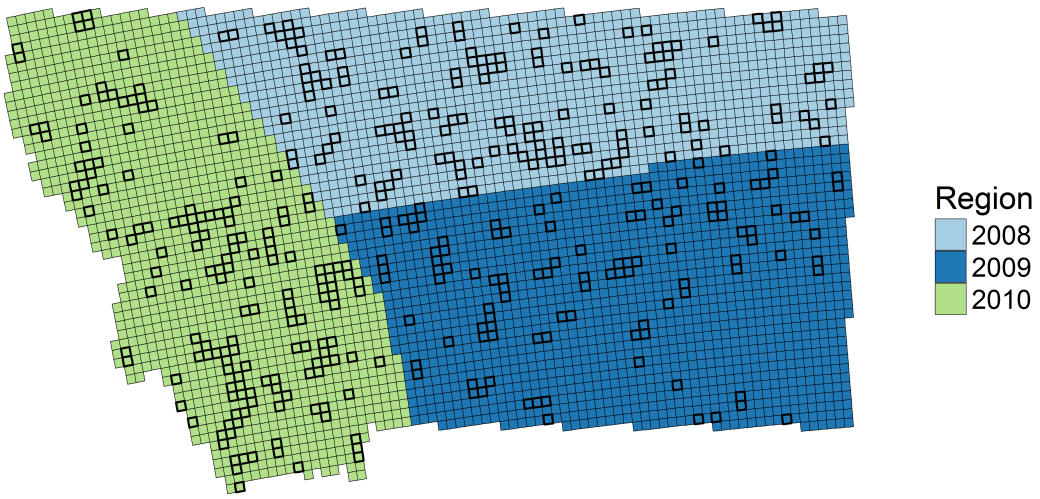

Figure 1: Grid cells from the North American Bat Monitoring Program that intersect the state of Montana. The color of each cell indicates which region it belongs to, with the thicker outline showing cells that had at least one visit. The regions were defined according to approximately where most of the sampling effort for each year was located. The holdout cells are not shown.

Table 1: The number of total visits to the 406 sample sites used in the analysis and the 199 holdout sites.

Total Visits	1	2	3	4	5	6	7	8	9	10	11	12	13-17
Sample Sites	114	87	69	37	17	9	16	18	12	10	5	9	3
Hold-out Sites	75	42	28	26	11	3	5	4	2	1	0	1	1

MYCA, MYCI, MYEV, MYVO; Maxell 2015). For the Montana bat species not included in our analysis, MYSE is known to be susceptible to WNS (Langwig, Frick, Reynolds, et al. 2015; Frick, Puechmaille, & Willis 2016) and the fungus has been detected on LABO (Bernard et al. 2015).

In order to estimate occupancy, sites must be defined where the probability of occupancy (at least one individual) within the site is the primary parameter of interest to be estimated by the model. Additionally, at least some of the sites must include multiple visits in order to estimate detection probabilities. Although these data were not collected following a pre-defined grid, we used the given geographic coordinates to associate each record with the 10 by 10 kilometer grid created for the North American Bat Monitoring Program (NABat; Loeb et al. 2015) and considered each grid cell a site when estimating occupancy. This results in multiple visits to a portion of the defined grid cells and data that is overall consistent with an occupancy framework. We delineated three regions across the state that denote where the majority of the surveys occurred each year (Figure 1). However, each year there was some overlap where, for instance, surveys from 2008 occurred in the other two regions we defined. For this analysis, we excluded any surveys that occurred outside the primary region for a given year and used these as holdout data during our model assessment. This resulted in a total of 406 sample sites (grid cells) with at least one visit and 199 sites for the holdout data. The total number of visits to each site ranged from 1 to 17 (Table 1) with 1455 total visits for the sampled sites and 541 total visits in the holdout set.

The Montana Natural Heritage Program also provided a set of covariates across the entire state. Each of these covariates was at a resolution of 90 by 90 meters. To be incorporated into

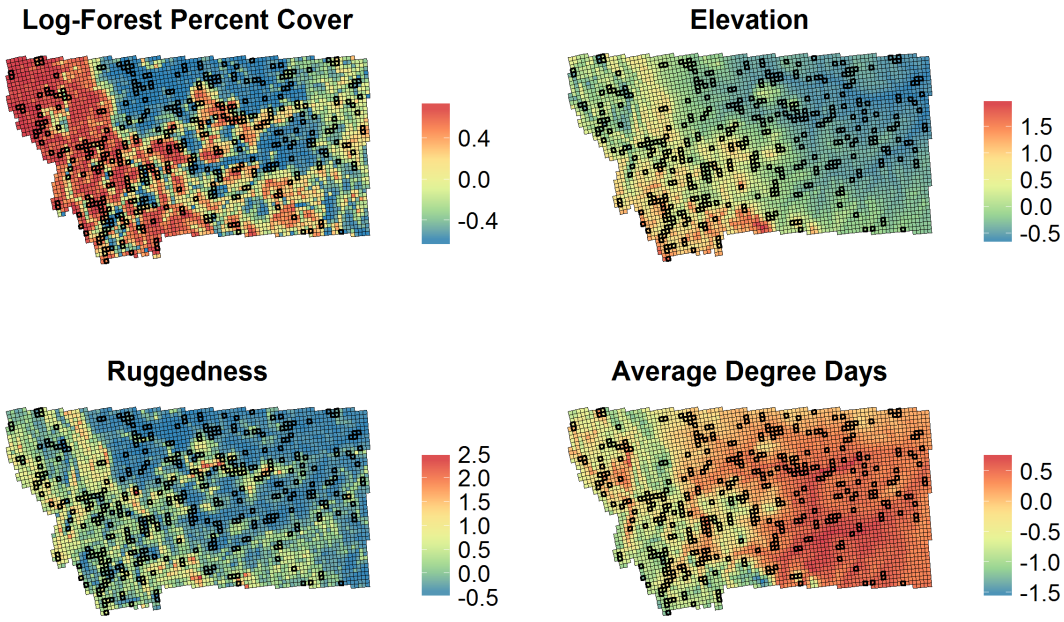

Figure 2: Maps of the log-transformed forest cover (%), elevation, ruggedness, and average degree days for each grid cell across the state. The scales show the centered and scaled covariate values used in the analysis. Cells with the thicker outlines show sites that had at least one visit.

the occupancy component of the model, these covariates needed to be associated with the sites defined for the analysis. For each covariate, we associated every value measured at the 90 by 90 meter scale to a site based on which 10 by 10 kilometer NABat grid cell its centroid was contained in. Then all of the covariate values included within a grid cell were averaged to obtain a site-level covariate. For instance, the average of all elevations recorded across a grid cell were averaged and this aggregated elevation measure was included as a covariate in the model. In this way, these site-level covariates can be included in the analysis to explain heterogeneity in the probabilities of occupancy and/or detection. The site-level covariates are also required to make spatial predictions for occupancy across the entire state. Although more covariates were available, we focused on using forest percent cover (log-transformed), elevation, ruggedness, and average degree days (Figure 2). These covariates are believed to be related to occupancy for many bat species and, except for average degree days, similar

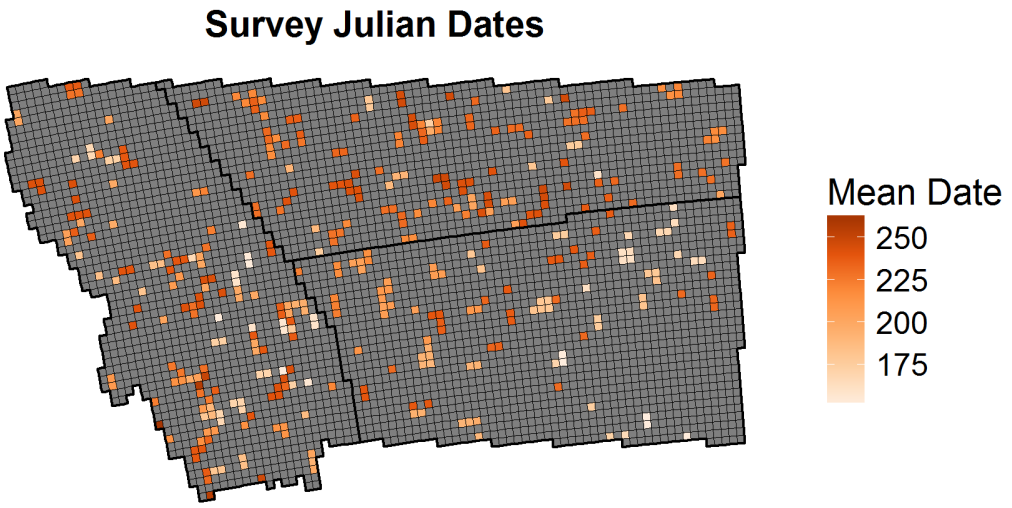

Figure 3: Mean Julian date across visits within each surveyed site. Gray grid cells were not visited and the holdout sites are not shown here. Thick black lines show the three regions we designated based on the different survey years.

covariates were used by Rodhouse, Ormsbee, Irvine, Vierling, et al. (2015) to model bat distributions in other western states. The forest percent cover variable was determined based on whether the land cover (at the 90 by 90 meter resolution) was classified as some type of forest or not. Elevation was recorded in meters above mean sea level. The vector ruggedness measurements (Sappington, Longshore, & Thompson 2007) quantify the ruggedness of an area and take on values between 0 and 1. The degree days covariate is the annual average number of days above 32 degrees Fahrenheit for 1981 to 2010. The distributions of these covariates within the sample sites appear representative of the variation across the state of Montana (Appendix Figure A1).

Within each site, we considered a single detection record (either acoustic or mist netting) for one night as a visit for this analysis. For each individual visit, available covariates included the detection method (mist netting or acoustic) and the date. Within each of the regions we defined, there is some spatial pattern in the mean Julian date of visits within the same grid cell (Figure 3). We accessed additional weather covariates using R (R Core Team 2017) with the packages `rnoaa` (Chamberlain 2017) and `countyweather` (Severson & Anderson

2016). Daily minimum temperature and daily precipitation values from the nearest available weather station were linked to each record. We attempted to obtain data on daily maximum wind speed as well, but found this information unreliable and inconsistently measured across many weather stations. These weather covariates are not ideal because there is obviously a large degree of spatial and temporal misalignment from the actual bat sampling period for each visit. However, we hoped that this information could be used to account for at least some of the heterogeneity in detection probabilities that is believed to be associated with these covariates due to differences in bat activity.

Model

For this analysis, we assume that sites $i = 1, \ldots, n$ are occupied by species $k = 1, \ldots, K$ with probability ψ_{ik} such that

$$Z_{ik} \sim \text{Bernoulli}(\psi_{ik}), \tag{1}$$

where Z_{ik} is an indicator for whether the species is present (1) or not (0). Here we have a total of $n = 406$ unique sites visited across Montana and $K = 8$ species. For each species, the probability of occupancy was modeled using a logit link with the log-transformed forest cover, elevation, ruggedness, and average degree days covariates for each site. That is, the probabilities in equation 1 are modeled as $\text{logit}(\psi_{ik}) = \mathbf{X}_i\boldsymbol{\beta}_k$ where $\mathbf{X}_i$ is a row vector of the covariates for site i and $\boldsymbol{\beta}_k$ is the vector of associated coefficients for species k. Except for MYCA, we assumed the ranges of all species included all of Montana and they could possibly occupy any site. In the analysis, we restricted observations for MYCA to include only the region sampled during 2010 ($n = 159$, Figure 1) based roughly on the known range of the species (although it could extend slightly further to the southeast of this region).

Conditional on site i being occupied by species k ($Z_{ik} = 1$), we model the detection process for visits $j = 1, \ldots, J_i$ as

$$Y_{ijk} \sim \text{Bernoulli}(p_{ijk}), \tag{2}$$

where p_{ijk} is the probability of detection and the species can either be detected ($Y_{ijk} = 1$) or not ($Y_{ijk} = 0$) on each visit. We denote the total number of visits to site i as J_i and it is allowed to vary across sites (Table 1). Similar to the occupancy probabilities, we let $\text{logit}(p_{ijk}) = \mathbf{V}_{ij}\boldsymbol{\alpha}_k$ where $\mathbf{V}_{ij}$ is a row vector of visit-level covariates for visit j at site i and $\boldsymbol{\alpha}_k$ is a vector of associated coefficients for species k. We included several visit-level covariates to model detection probabilities in equation 2: an indicator for whether the record was an acoustic detector (1) or not (0; mist netting), Julian date, a quadratic term for Julian date, minimum daily temperature, and an indicator for whether there was any precipitation (1) or not (0) on that date. The quadratic term for Julian date was included based on the idea that bat activity, and therefore detection probability, is likely highest in the middle of the summer and lower otherwise. This pattern in detection probabilities has been found in bat species (Pauli, Zollner, & Haulton 2017) and could be accounted for with the quadratic term for Julian date. Similar to the occupancy covariates, all of the visit-level covariates were centered and standardized prior to including them in the model. In this case, the intercept term for the detection model corresponds to mist netting on a date with no precipitation and average values for the Julian date and minimum temperature covariates.

We also added a hierarchy for each fixed effect that allowed information to be borrowed across each species (i.e., using a 'community-level prior distribution'; Zipkin, Campbell Grant, & Fagan 2012). For each species (k), the model includes $g = 1, \ldots, 5$ fixed effect coefficients for occupancy (β_{gk}) and $h = 1, \ldots, 6$ fixed effect coefficients for detection (α_{hk}). In the earlier descriptions, we represented these same coefficients as vectors for each species where, for instance, $\boldsymbol{\beta}_k' = [\beta_{1k}, \beta_{2k}, \beta_{3k}, \beta_{4k}, \beta_{5k}]$. This added hierarchy assumes that for a particular covariate the associated coefficients across different species come from a common distribution. Therefore, we let $\beta_{gk} \sim \text{Normal}(\mu_{\beta_g}, \sigma^2_{\beta_g})$ and $\alpha_{hk} \sim \text{Normal}(\mu_{\alpha_h}, \sigma^2_{\alpha_h})$ where the μ and σ^2 parameters are the means and variances, respectively, for each 'batch' of coef-

ficients. Note that in this structure, a batch of coefficients represents the set of relationships across the different species between a single covariate (i.e., elevation) and probability of interest (on the logit scale). This hierarchy across species makes sense because we often expect similar relationships between covariates and the probabilities of occupancy and/or detection. For example, Rodhouse, Ormsbee, Irvine, Vierling, et al. (2015) found that generally detection probabilities were higher for acoustic detectors than for mist netting. Our model structure can take advantage of this pattern by borrowing information across species to result in more precise estimates of these coefficients. The structure is still flexible, however, and will also allow for differences among species if the data do not provide evidence of a similar relationship across species for a particular covariate. We initially fit this model to these data assuming occupancy among sites and detections among visits (conditional on site occupancy) were both independent.

Based on the spatial configuration of the sampled sites (Figure 1), we then considered the possibility of spatial correlation in the probabilities of occupancy following an approach similar to Johnson et al. (2013). However, based on residual patterns observed after fitting the first model (assuming independence), we also fit a model with spatial correlation in the probabilities of detection (but no correlation for occupancy). The following briefly describes incorporating the spatial random effects for the occupancy process. We structured the spatial random effects in the same way when fitting a model with spatial correlation among detection probabilities. Briefly, these random effects were parameterized to result in an intrinsic conditionally autoregressive (ICAR) spatial correlation structure. The ICAR random effects were restricted to ensure that they were orthogonal to the fixed effects previously described for occupancy (i.e., $\mathbf{X}$). In matrix form, this results in the logit of the probability of occupancy for species k being defined as

$$\text{logit}(\boldsymbol{\psi}_k) = \mathbf{X}\boldsymbol{\beta}_k + \boldsymbol{\eta}_k, \tag{3}$$

where $\boldsymbol{\eta}_k$ is a vector of the spatial random effects for species k. Overall, this allows the

inclusion of fixed effects (that have some spatial structure themselves) to explain patterns in occupancy while the spatial random effects can account for any remaining spatial correlation in occupancy probabilities that is left unexplained. Again, the idea is the same when incorporating spatial correlation for detection by adding a site-level random effect to the probabilities on the logit scale.

Following Johnson et al. (2013), we defined these random effects as follows. Let $i = 1, \ldots, N$ represent all sites (both visited and unvisited) across Montana with covariate matrix $\mathbf{X}$. Then the $N \times N$ association matrix $\mathbf{A}$ is composed of values indicating whether sites i and i' are neighbors (1) or not (0) for each element $A_{ii'}$. Using $\mathbf{P}^{\perp} = \mathbf{I} - \mathbf{X}(\mathbf{X}'\mathbf{X})^{-1}\mathbf{X}'$, the residual projection matrix of $\mathbf{X}$, the Moran operator matrix is defined as $\mathbf{\Omega} = N\mathbf{P}^{\perp}\mathbf{A}\mathbf{P}^{\perp}/(\mathbf{1}'\mathbf{A}\mathbf{1})$. Here, $\mathbf{I}$ represents an identity matrix and $\mathbf{1}$ is a vector of all ones. The eigenvectors of $\mathbf{\Omega}$ describe an ICAR spatial correlation structure across all sites in a form that is independent of the fixed effects. Most of this spatial correlation structure can be represented in a restricted (reduced number of parameters) form with the matrix $\boldsymbol{\kappa}$ composed of the first q eigenvectors of $\mathbf{\Omega}$. For this analysis, we defined the spatially restricted random effects for species k to be $\boldsymbol{\eta}_k = \boldsymbol{\kappa}\boldsymbol{\theta}_k$ with $q = 200$. The vector of parameters $\boldsymbol{\theta}_k$ are specified to follow a multivariate normal distribution with mean vector $\mathbf{0}$ and variance-covariance matrix $\nu_k^2\mathbf{\Sigma}$. To define $\mathbf{\Sigma}$, first we specify $\mathbf{D}$ as a diagonal matrix with each element D_{ii} equal to the total number of neighbors for site i and matrix $\mathbf{Q} = \mathbf{D} - \mathbf{A}$. Then let $\mathbf{\Sigma} = (\boldsymbol{\kappa}'\mathbf{Q}\boldsymbol{\kappa})^{-1}$. Each species also has an associated scaling parameter represented by ν_k^2 for species k. Further details on restricted spatial regression models can be found in Hughes & Haran (2013) or Johnson et al. (2013) for specific application to occupancy models.

We used R (R Core Team 2017) to conduct this analysis and fit this model using a Bayesian approach with Stan (Carpenter et al. 2016) called from R using the rstan package (Stan Development Team 2016). For the fixed effects, we specified independent Cauchy(0, 2.5) and Half-Cauchy(0, 2.5) prior distributions for means (μ) and variances (σ^2), respectively, of the batches of coefficients. For the spatial random effects, we used

Half-Normal$(0, 25)$ prior distributions for the scaling parameters (ν) for each species. We summarized the posterior distribution using four chains of 1000 iterations each after the first 1000 iterations from each chain were discarded as a burn-in. Model convergence was assessed by examining traceplots to ensure chains showed good mixing and by checking that potential scale reduction factors ($\hat{R}$) for each parameter were less than 1.05 (Brooks & Gelman 2012).

Model Assessment

We assessed this occupancy model using residual diagnostics and receiver operating characteristic curves. Residual plots were examined to assess whether important covariates or covariate structure were excluded from the model. For each species, we examined residual plots for both the detection and occupancy components of the model. Any strong patterns suggest that additional model structure needs to be included to explain unaccounted for heterogeneity in the probabilities of interest. For the occupancy component of the model, we examined residual plots versus the covariates included in the model as well as the additional site-level covariates that were provided by the Montana Natural Heritage Program.

We also used these residuals to construct spatial correlograms for both occupancy and detection. If the independence assumptions for both of these processes are correct, we would expect no spatial correlation to be present in the residuals grouped by distance classes. We described the uncertainty in the spatial correlograms over the posterior distribution of the parameters by constructing 95% credible intervals (CIs) for each species. These plots can be interpreted by examining whether the resulting bands include zero for every distance class, which would be expected if the assumptions of the model are adequately met. We examined new spatial correlograms of the residuals after fitting the models that included spatial correlation for occupancy or detection.

The predictive characteristics of the fitted models were assessed using the area under the receiver operating characteristic curves (AUC). We performed this assessment using a holdout sample and also, separately, the in-sample observations used to fit the model. The holdout observations occurred outside the regions we defined (Figure 1) during each respec-

tive primary year. For each species, we calculated separate AUC values for the detection process and the occupancy process at each saved iteration (Zipkin, Campbell Grant, & Fagan 2012). This summarizes predictive performance across both levels of the model and also accounts for the posterior uncertainty in each parameter. Values for AUC can range from zero to one with higher values indicating better predictive performance. An intercept-only model without any predictors is expected to have an AUC of 0.5 which is typically considered poor predictive performance.

Spatial Predictions

Inferences from this model are primarily summarized with maps depicting the predicted probabilities of occupancy and associated uncertainty for all cells across Montana. We predicted occupancy probabilities using the site-level covariates in the model along with the posterior distributions of the associated fixed effect coefficients. Therefore, these maps show the unconditional probabilities, meaning we do not describe sites with at least one detection as having an occurrence probability of one. For each species we present two maps: the first shows the posterior mean of the predicted probabilities of occupancy as an estimate and the second shows the width of the 95% CIs at each site as a measure of the uncertainty. We predicted MYCA occurrence probabilities only for the 2010 region based on its assumed range, but the occupancy probabilities for the remaining species are predicted across the entire state. Maps were also created for combinations of species to represent the estimated probability and associated uncertainty of all species within a group being present at a grid cell. It should be noted that predictions in these maps assume that, after accounting for the covariates included in the model, unsampled sites are not systematically different than the sampled sites. We are not aware of the exact sampling design used when collecting these data and this could impact inferences. For instance, if sites were selected based on prior knowledge that bats likely occupy the area, then occupancy predictions would likely be positively biased.

While we refer to the predicted probabilities as "occupancy", the inferences might be

better described as "use". This is in part because acoustic detections and mist netting captures only provide evidence of bat species using a location but not how it is used (i.e., if roosting in, feeding in, or traveling through the grid cell). Additionally, with highly mobile species, the closure assumption of occupancy models is more likely to be violated but generally only impacts the interpretation of estimates (Kéry & Royle 2016). In this case, estimates represent the probability of the species using each grid cell for at least part of the defined summer period. We will continue to refer to all of the estimates as occupancy for simplicity.

Results

Spatial Correlation Patterns

We first assessed potential spatial correlation patterns using the residuals of the first model fit that assumed independence for both the occupancy and detection components. For occupancy, the 95% CI bands of the spatial correlograms include zero across all distances, providing no evidence of unexplained spatial correlation (Appendix Figure A2). The spatial correlograms based on the detection residuals, on the other hand, consistently provide evidence of correlation among residuals at shorter distance classes (Appendix Figure A3). Fitting a model with spatial correlation only for the occupancy process, as we originally suspected may be needed, did not change these patterns in the spatial correlation of the residuals (results not shown). However, the model with spatial correlation for detections does appear to resolve these patterns and shows no strong trends in the spatial correlograms for any of the species in this analysis (Appendix Figures A4, A5). Based on this assessment, the remaining results focus on this model (spatial correlation for detection) and we used it to generate the maps of predicted occupancy. This model includes the same fixed effect structures previously described for detection and occupancy.

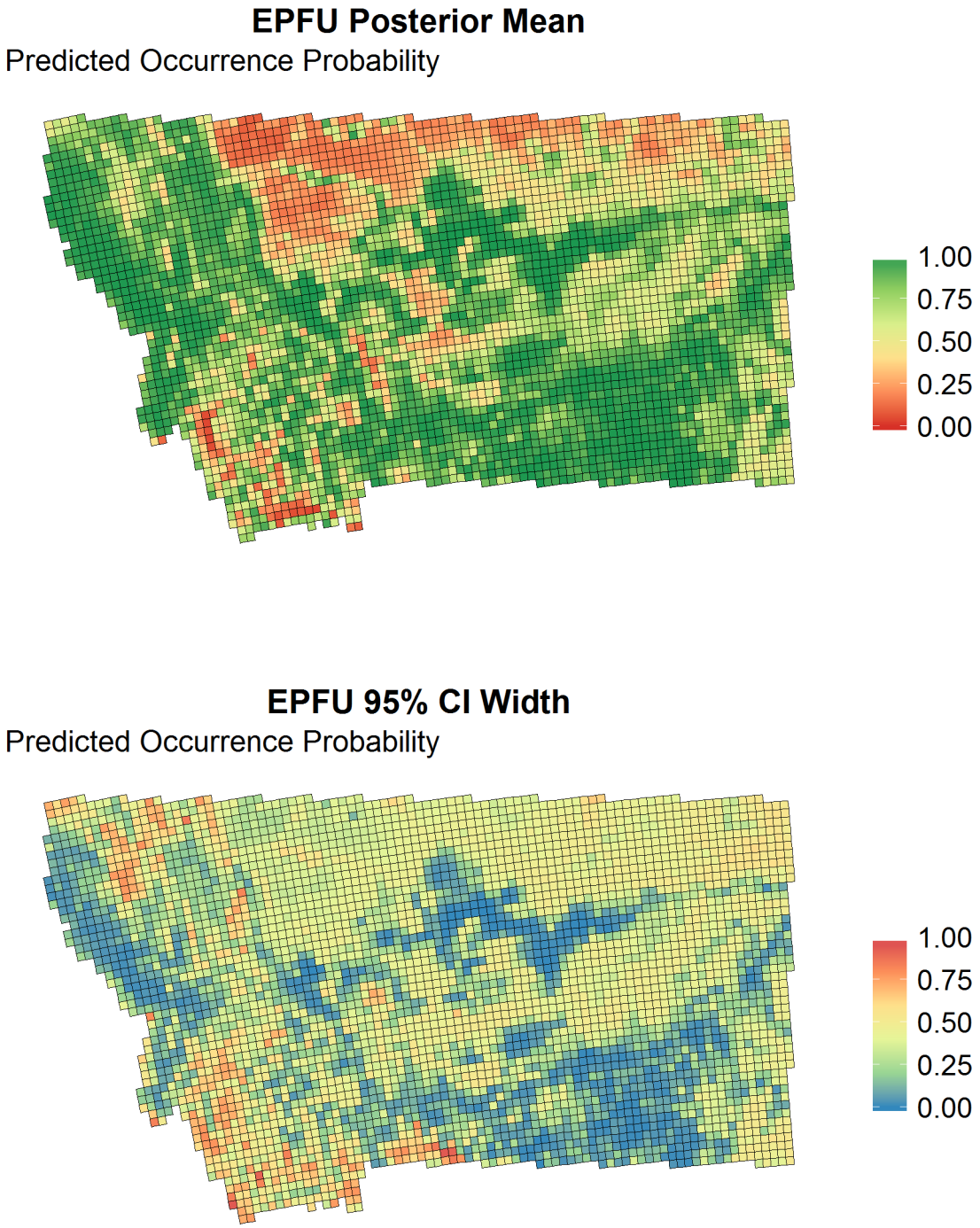

Figure 4: For EPFU, map showing the predicted probability of occupancy for sites across Montana and the associated uncertainty.

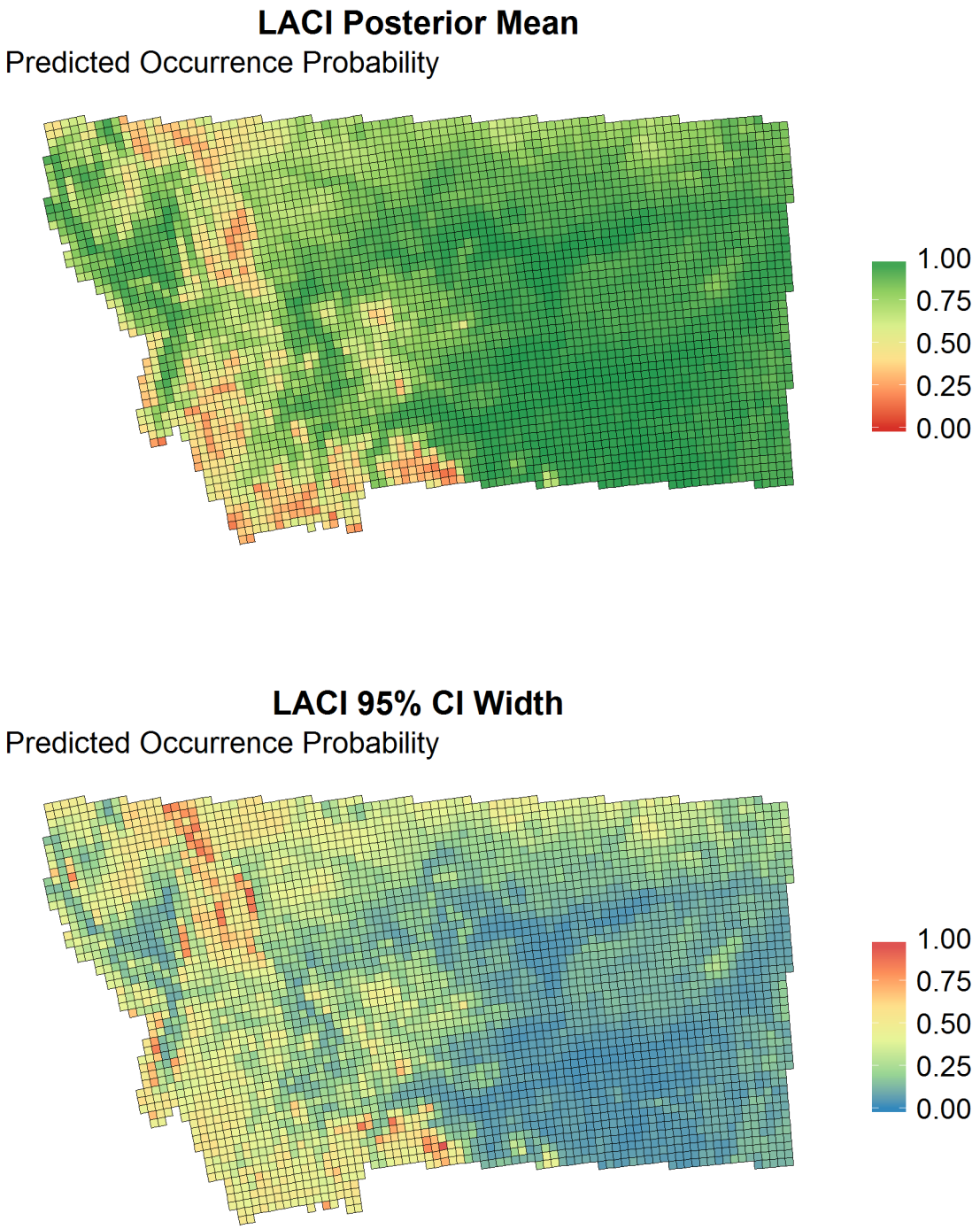

Figure 5: For LACI, map showing the predicted probability of occupancy for sites across Montana and the associated uncertainty.

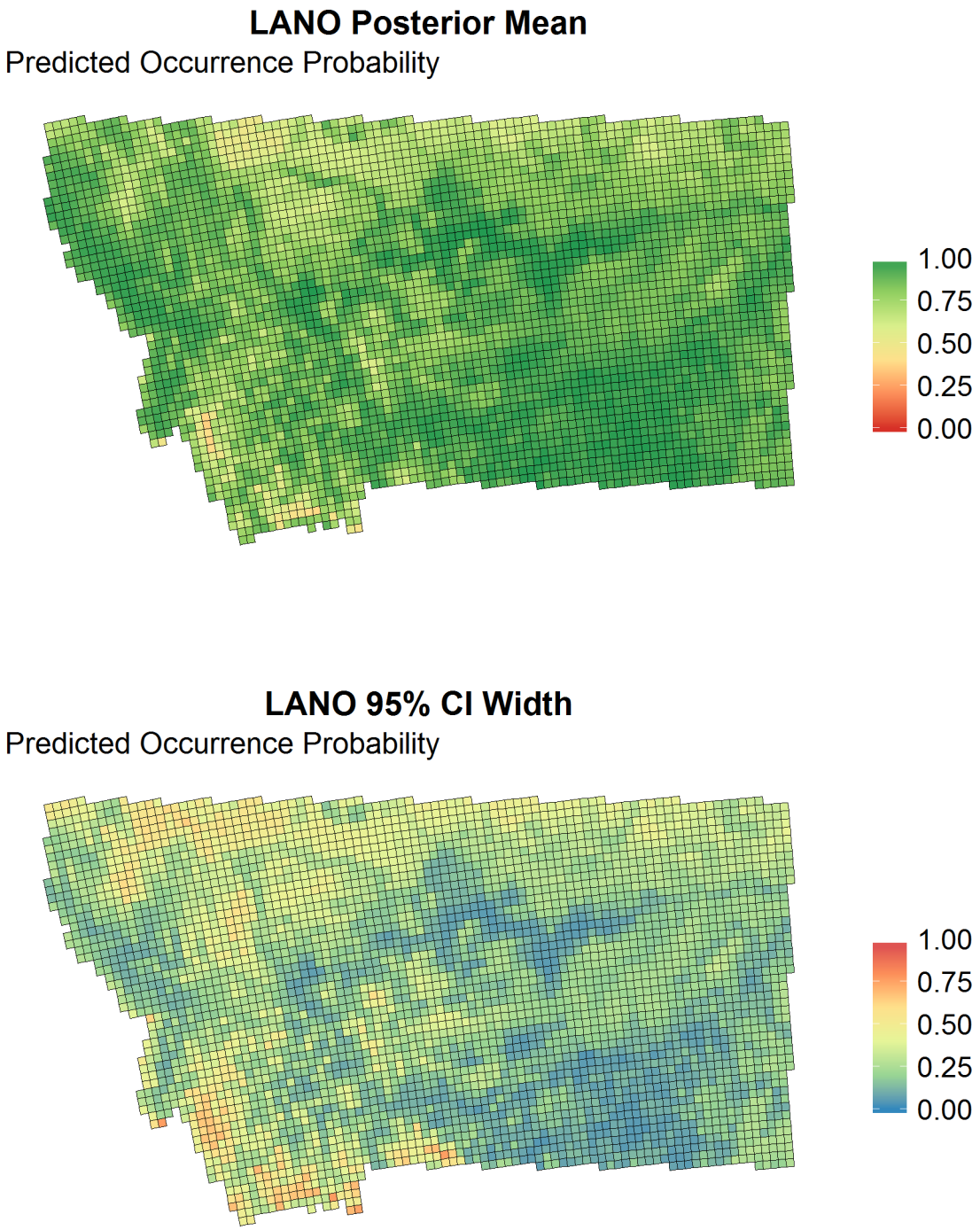

Figure 6: For LANO, map showing the predicted probability of occupancy for sites across Montana and the associated uncertainty.

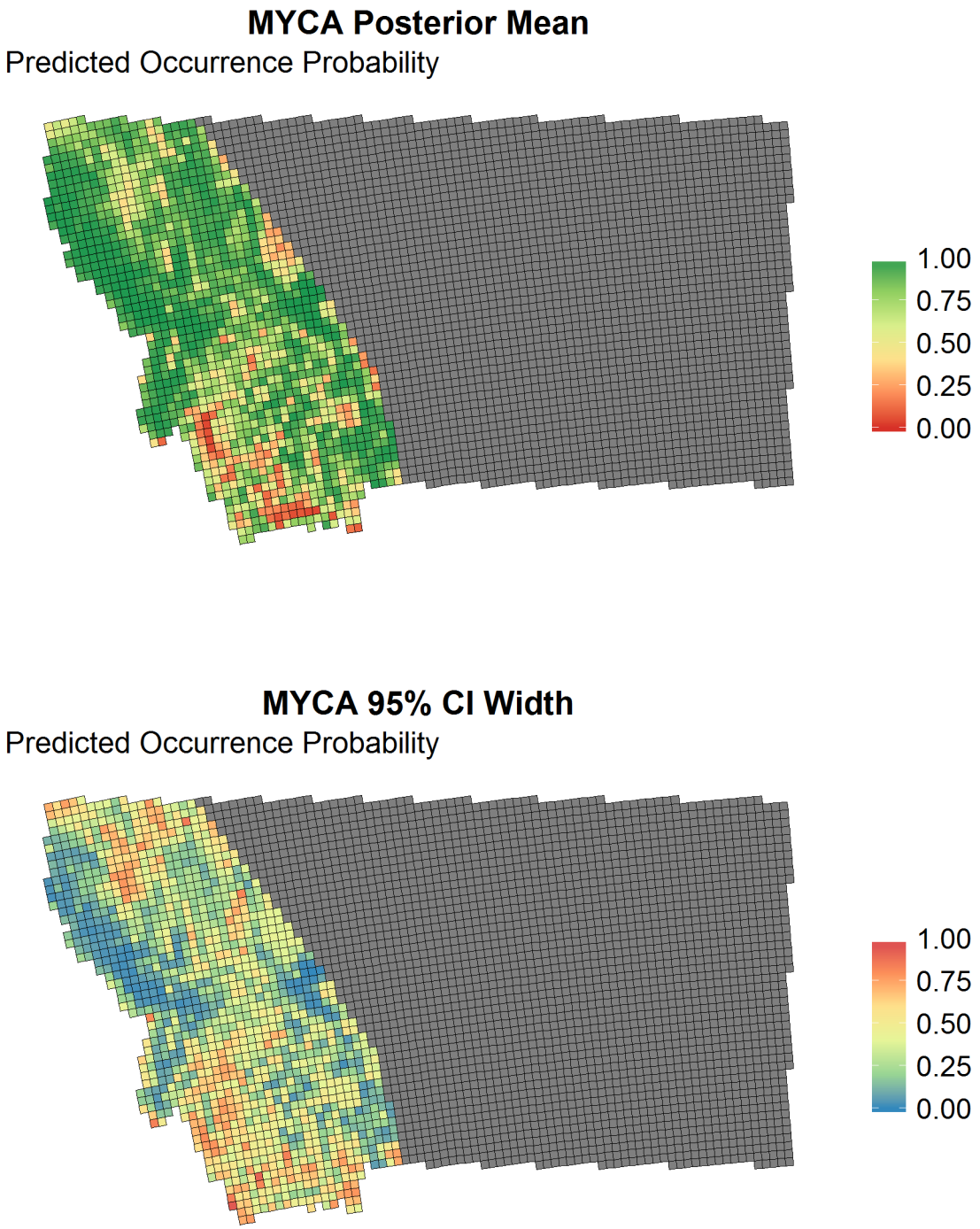

Figure 7: For MYCA, map showing the predicted probability of occupancy for sites approximately within its range across Montana and the associated uncertainty.

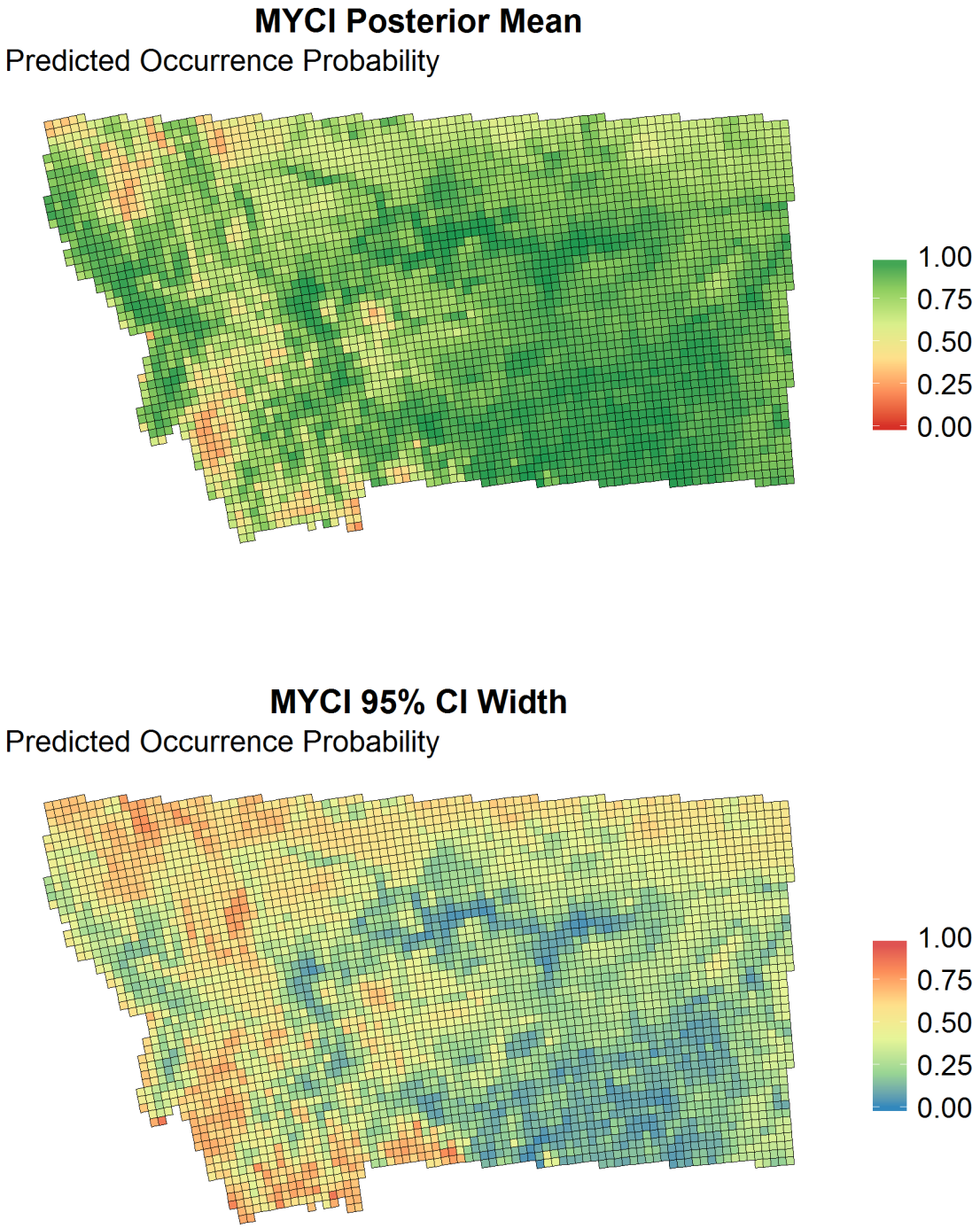

Figure 8: For MYCI, map showing the predicted probability of occupancy for sites across Montana and the associated uncertainty.

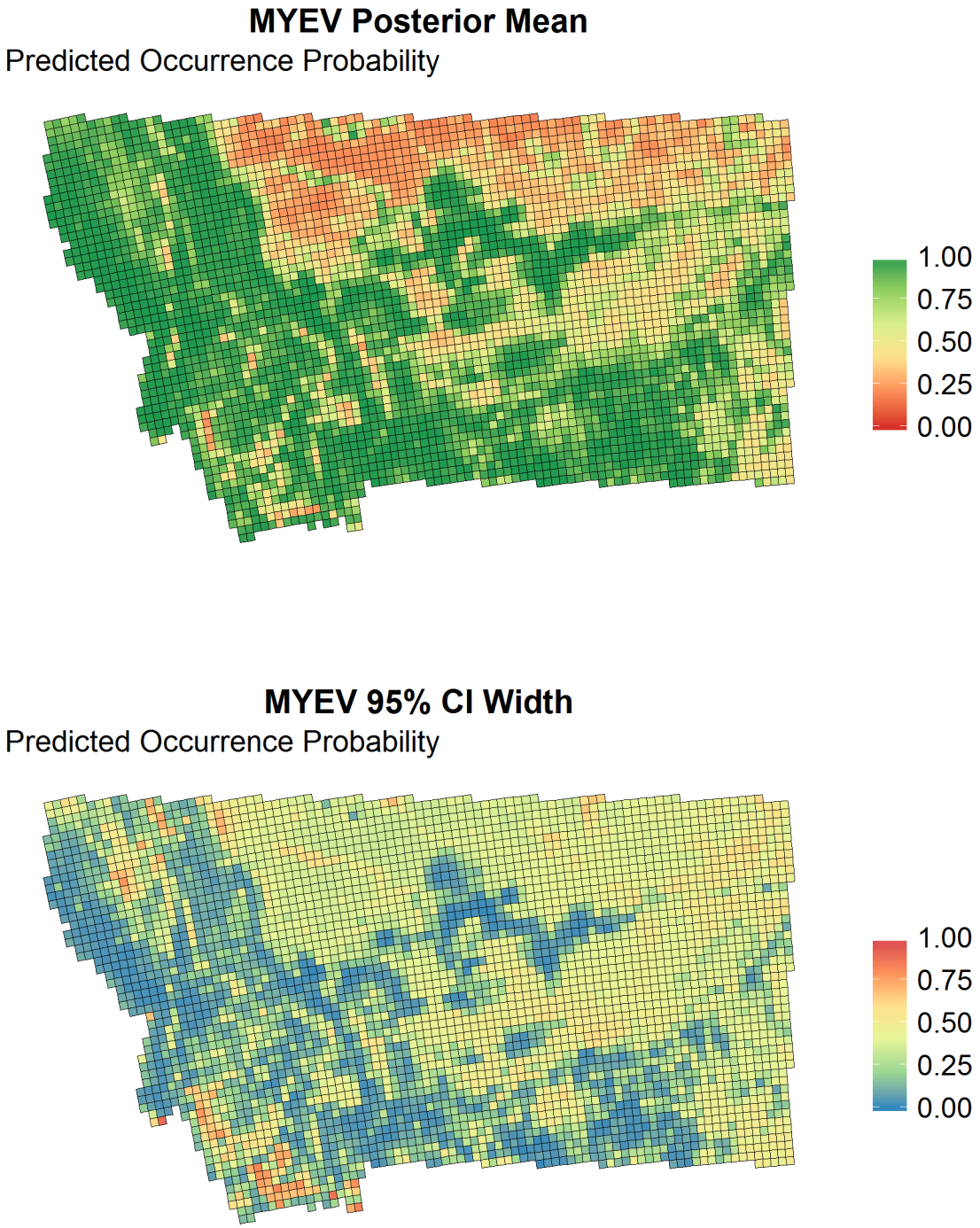

Figure 9: For MYEV, map showing the predicted probability of occupancy for sites across Montana and the associated uncertainty.

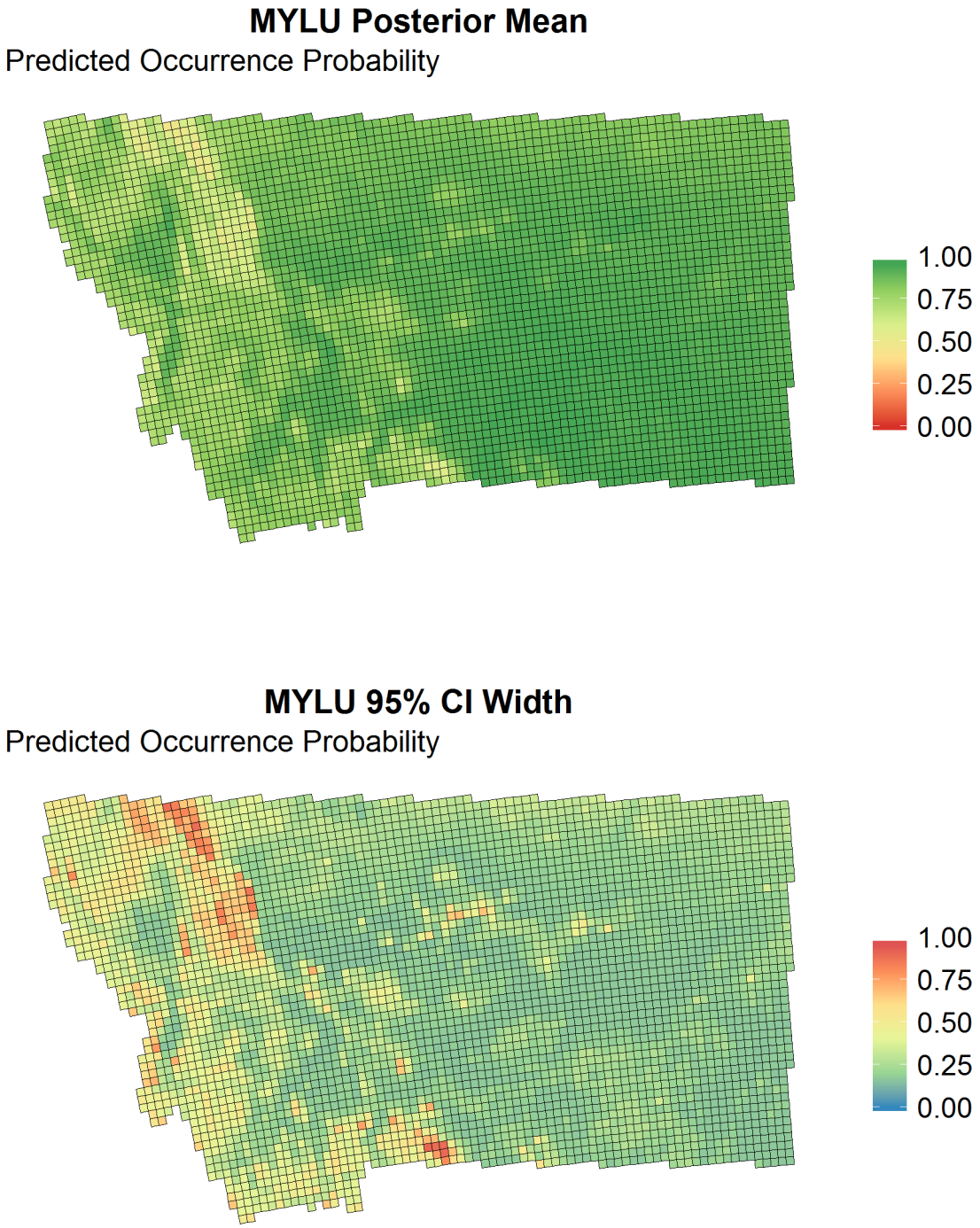

Figure 10: For MYLU, map showing the predicted probability of occupancy for sites across Montana and the associated uncertainty.

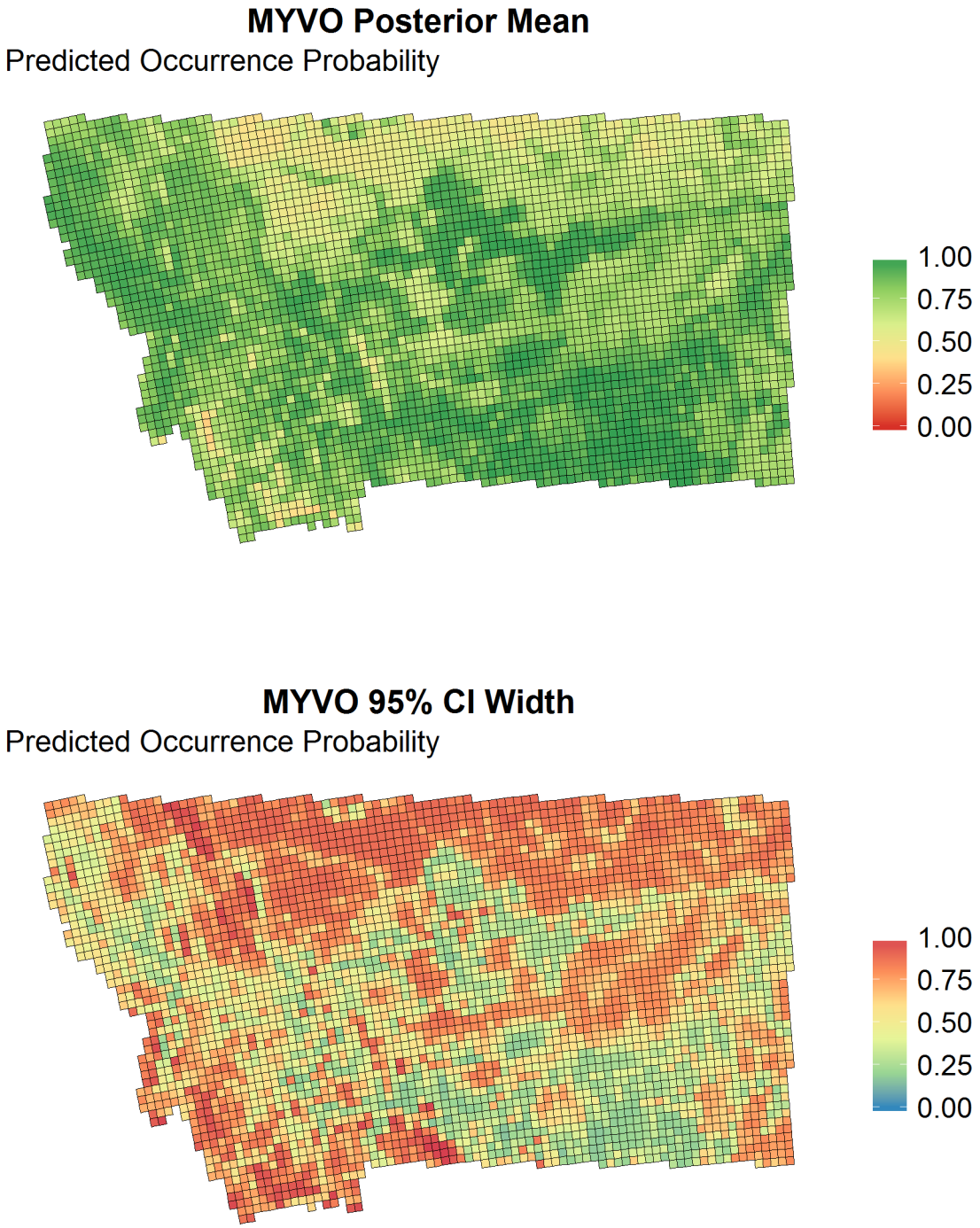

Figure 11: For MYVO, map showing the predicted probability of occupancy for sites across Montana and the associated uncertainty.

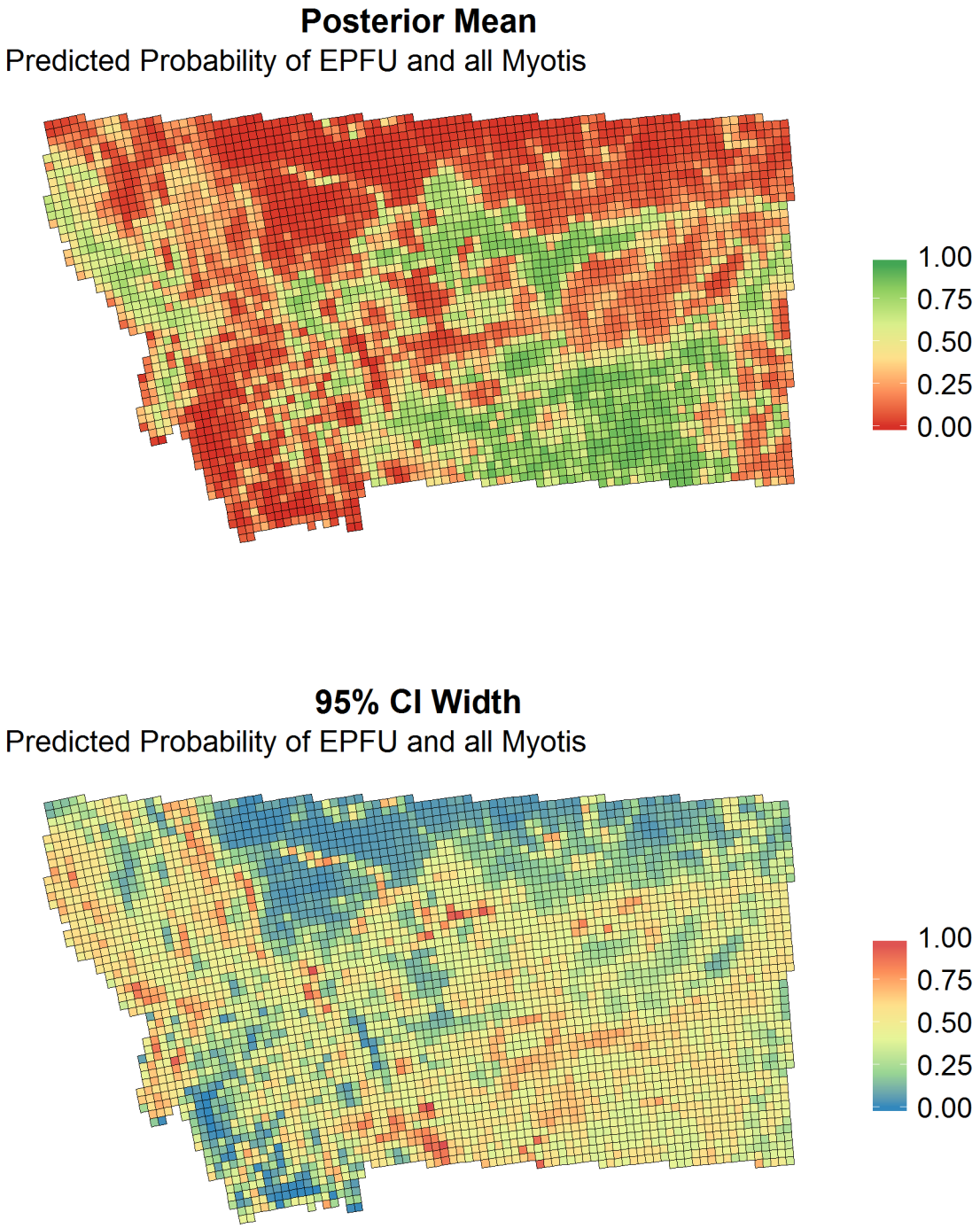

Figure 12: Estimated joint probabilities of occupancy for EPFU and all *Myotis* species at sites across Montana. The estimates correspond to the probability that all these species are present within a grid cell and the associated uncertainty.

Species Distribution Maps

We summarize the results of this model fit using maps of the predicted probabilities of occupancy for each species (Figures 4-11). Many species have large areas of the state with high predicted probabilities of occupancy, based on the posterior means. For instance, MYLU has generally high predicted probabilities of occupancy across the entire state with no strong patterns (Figure 10). The uncertainty in the spatial predictions varies by species and appears largest for MYVO (Figure 11). We also used the model to estimate the joint probability of occupancy for EPFU and all *Myotis* species at each grid cell (Figure 12). This map shows the estimated probability of all these species being present within a grid cell and the associated uncertainty. In this case, the map and predicted probabilities are mainly impacted by EPFU and MYEV because those species have the most grid cells with low estimated occupancy probabilities across the state. We created joint occupancy maps for other species combinations including all species in this analysis (Appendix Figure A6), EPFU and MYLU (Appendix Figure A7), and all *Myotis* species in this analysis (Appendix Figure A8).

The spatial predictions for occupancy are based on the posterior distributions of the occupancy coefficients (Appendix Figure A9). There were generally positive intercept coefficients representing higher probabilities of occupancy for most species when covariates are at their average values. Many species also have positive coefficients for the forest covariate (although the 95% CIs include zero for all except EPFU and MYEV) which is likely resulting in some of the patterns in the predicted maps that are similar across species (i.e., compare to the map of log-forest cover in Figure 2). The posterior distributions generally show a lot of uncertainty for each parameter that is leading to the high uncertainty in some areas of the predicted maps. The wide intervals for the occupancy coefficients are related to the coefficients for detection (Appendix Figure A10) as well as the within-site sampling scheme. The posterior distribution of the detection intercept coefficient is negative for every species with most posterior means around -3 for this parameter. This indicates low detection proba-

bilities, on average, for mist netting. While most species have higher detection probabilities for the acoustic detectors ('Pett' coefficients with generally positive posterior distributions; Appendix Figure A10), detection is still fairly low overall. Of the eight species we focused on, only MYVO had evidence that acoustic detection probabilities are lower than those for mist netting and as a consequence had the most uncertainty in the predicted occupancy map. The combination of low detection probabilities and few visits to most sites (Table 1) results in large uncertainty in the occupancy parameters.

Johnson et al. (2013) use the posterior distribution of the scaling parameter for the spatial random effects as evidence for spatial correlation if it is 'sufficiently far from zero' (pg. 805). For all species except MYVO, the 95% CIs of these parameters from the model with spatial correlation for detection are greater than one (Appendix Figure A11). This provides further evidence of spatial correlation among detections for these species. The high uncertainty associated with the spatial scaling parameter for MYVO is likely tied to the overall low detection probabilities for this species.

Model Assessment

The residual plots from an initial model fit showed no obvious patterns left unexplained in the occupancy structure of the model. This does not necessarily ensure adequacy of the occupancy portion of the model, as it is likely there are additional, but unknown, covariates related to the probabilities of occurrence for each species. For detection, the indicator for precipitation was originally excluded from the model, but residual plots suggested it could be an important predictor for some species. As a result, this covariate was included in the final model we present here. As previously described, we also used spatial correlograms of the occupancy and detection residuals to assess the evidence for spatial correlation in this model.

We used posterior distributions of both the out-of-sample and in-sample AUCs to compare the predictive performance of the independent, spatial correlation for occupancy, and spatial correlation for detection models. For each species, we examined these summaries for both

the detection process (using the y_{ijk} values themselves) and the occupancy process (using the posterior distribution of the latent z_{ik} values). The in-sample AUCs for detection based on the model with spatial correlation for detection were much higher than the other two models (Appendix Figure A12). This pattern is not seen in the posterior distributions of the out-of-sample AUCs where the values generally indicated mediocre to poor predictive performance (posterior means 0.5-0.6). Some species (MYCA, MYEV) even have detection AUCs less than 0.5 which is indicating very poor predictive performance of the detection component of the model. For occupancy, on the other hand, there is generally evidence of good predictive performance for all species, where the posterior mean AUC are mainly around 0.8 and are similar across the three models we explored (Appendix Figure A12).

Discussion

We analyzed detection/non-detection data for eight bat species in Montana to create species distribution maps based on a hierarchical community occupancy model. We focused on three years of data (2008, 2009, and 2010) with the most total records in order to better meet the general assumptions of this approach. The model also accounted for spatial correlation in detection probabilities within each species using restricted spatial random effects. The resulting species distribution maps show the posterior mean predicted probability of occupancy across the state and can be used as a baseline reference for comparing to future maps. Changes in species' distributions after the arrival of WNS could be better understood and assessed by comparing future distribution maps to these baselines. Future analyses could also estimate occupancy for each species in a multiple season model that could directly estimate changes in the probability of occupancy for each species (Rodhouse, Ormsbee, Irvine, Vierling, et al. 2015). Additionally, the estimated coefficients for detection and occupancy from this model can help inform the sampling design for the monitoring program moving forward. This could include providing guidance on sampling design in terms of number of visits needed per site in order to reduce uncertainty in distribution maps or by focusing WNS surveillance efforts on areas of high occupancy probabilities for at risk species.

There are a few obvious drawbacks to this analysis. First, there was generally very high uncertainty in the occupancy coefficients of the model which led to high uncertainty in spatial predictions for areas of each map. This issue is not necessarily surprising based on the within-site sampling design and overall low detection probabilities for these bat species. Precision in occupancy models can be improved with a survey design that includes an optimal number of visits to each site, depending on the detection and occupancy probabilities (MacKenzie & Royle 2005). When detection probabilities are less than one, MacKenzie & Royle (2005) show that a single visit to even a portion of sites is not ideal and instead they generally recommend at least three visits to each site. This recommendation assumes detection probabilities are at least 0.5, so even more visits are recommended for lower detection probabilities. The uncertainty in the predicted occupancy maps could be reduced with a different within-site sampling design that ensures each site has roughly the same number of visits. For example, spreading visits more evenly across the same 406 grid cells in this analysis would result in half with three visits each and half with four visits each, while keeping the total number of survey nights (across all grid cells) roughly the same. While is may seem counterintuitive, fewer sites with more visits to each could improve precision because of the generally low detection probabilities for bats. These issues and more concrete advice on planning bat surveys to estimate occupancy will be the focus of future work.

The second main drawback of this analysis is that, based on the posterior distributions of the out-of-sample AUCs, the predictive performance of the detection component of the model was poor. As shown in other analyses (e.g., Rodhouse, Ormsbee, Irvine, Vierling, et al. 2015), acoustic detection probabilities were higher than those for mist netting in most species. The remaining covariates in the model (date, minimum temperature, indicator for precipitation) are generally less informative for explaining heterogeneity in detection probabilities. The weather covariates are poorly aligned, both spatially and temporally, with the actual nights surveyed. Collecting this same weather information directly at surveyed locations for each night would be more ideal for modeling detection. Additionally, there

are likely other covariates at survey locations (e.g., some measure of vegetation clutter) that likely influence detection probabilities. Incorporating these additional covariates and better aligned weather covariates in the detection component of the model could greatly improve the associated predictive performance. Accounting for these sources of unexplained heterogeneity in detection probabilities could also improve estimation of occupancy. The posterior distributions of the AUCs for occupancy already show generally good predictive performance for this component of the model. It should be noted, however, that occupancy and detection are inherently linked in the model, so in some ways poor performance of one component should influence the other component as well. There is likely more research needed on evaluating the predictive performance of occupancy models in general, given the drawback of using AUC (Jiménez-Valverde 2012) and the uncertainty about how to interpret AUC values when the maximum possible AUC is less than one (Zipkin, Campbell Grant, & Fagan 2012).

After assuming independence in both the occupancy and detection components of the model, we explored the possibility of spatial correlation using correlograms of the residuals. These generally provided evidence of spatial correlation in detection probabilities but not for occupancy probabilities. Incorporating the spatial random effects for detection greatly improved the in-sample AUCs for detection (but there is still likely a need to collect additional detection covariates, as noted previously). Although we formulated the random effects with a spatial structure, there is also likely a temporal component to the correlation structure as well. The visits within nearby grid cells were generally collected around similar dates each year (Figure 3). While this ensures data collection is logistically feasible, it makes determining the cause of the correlated detection probabilities more difficult. Bat activity patterns often appear clustered in time (Hayes 1997; Fischer et al. 2009) and likely lead to correlated detection probabilities over consecutive nights (Wright, Irvine, & Rodhouse 2016). These "runs" in activity could also explain the evidence of spatial correlation among detection probabilities in these data because sites that are closer together were also visited

at similar times. This may be one explanation for why the spatial correlation for detection improved the predictive performance for the in-sample visits but not the out-of-sample visits. Ignoring correlation among detections can lead to negatively-biased estimates of occupancy. Compared to the model assuming independence, occupancy was estimated to be slightly higher for all species when we accounted for correlation among detections.

Additional bat species in Montana were not included in this analysis because they each had very few total detections (both in the primary years we focused on and across all available data). These species are generally much harder to detect and/or have very reduced ranges within the state. The much lower detection and occupancy probabilities make it difficult to estimate model parameters, although the multiple species hierarchy we included here can help address this issue. Incorporating some surveys that focus on these species in particular could help ensure there is an adequate number of detections for reliably estimating occupancy. Then, as done for MYCA, estimation and prediction would need to be restricted for the range of each species individually. Being able to incorporate additional species in future analyses would be beneficial because many of the species we excluded also are potentially susceptible to WNS.

Future Directions

As previously described, additional acoustic records are also available in Montana from a statewide network of long-term detector deployments. We plan to analyze these data with the aim of modeling bat activity while accounting for misidentifications. Changes in activity for affected species occur after the arrival of WNS (Ford et al. 2011) and monitoring activity could provide another source of information to aid in the early-detection of WNS in the state. The more in-depth analysis of bat activity could provide additional information on bat detection probabilities as well. Along with the detection estimates from the current analysis, this could be used to provide more guidance on designing future sampling efforts. We plan on providing simulations to explore how different sampling plans could be used to estimate changes in occupancy and/or activity over time.

Acknowledgments

We thank L. Hanauska-Brown, J. Gude, B. Maxell, D. Bachen, and B. Burkholder for their helpful discussions about this manuscript. Data were collected by Montana Fish, Wildlife, and Parks and their partners.

References

Bernard, R. F., Foster, J. T., Willcox, E. V., Parise, K. L., & McCracken, G. F. (2015) Molecular detection of the causative agent of white-nose syndrome on Rafinesque's big-eared bats (*Corynorhinus rafinesquii*) and two species of migratory bats in the southeastern USA. *Journal of Wildlife Diseases*, **51**.2, 519–522.

Brooks, S. P. & Gelman, A. (2012) General methods for monitoring convergence of iterative simulations. *Journal of Computational and Graphical Statistics*, **7**.4, 434–455.

Carpenter, B., Gelman, A., Hoffman, M., Lee, D., Goodrich, B., Betancourt, M., Brubaker, M. A., Guo, J., Li, P., & Riddell, A. (2016) Stan: A probabilistic programming language. *Journal of Statistical Software*.

Chamberlain, S. (2017) *rnoaa: 'NOAA' Weather Data from R*. R package version 0.7.0. URL: `https://CRAN.R-project.org/package=rnoaa`.

Fischer, J., Stott, J., Law, B. S., Adams, M. D., & Forrester, R. I. (2009) Designing effective habitat studies: quantifying multiple sources of variability in bat activity. *Acta Chiropterologica*, **11**.1, 127–137.

Ford, W. M., Britzke, E. R., Dobony, C. A., Rodrigue, J. L., & Johnson, J. B. (2011) Patterns of acoustical activity of bats prior to and following white-nose syndrome occurrence. *Journal of Fish and Wildlife Management*, **2**.2, 125–134.

Frick, W. F., Pollock, J. F., Hicks, A. C., Langwig, K. E., Reynolds, D. S., Turner, G. G., Butchkoski, C. M., & Kunz, T. H. (2010) An emerging disease causes regional population collapse of a common North American bat species. *Science*, **329**.5992, 679–682.

Frick, W. F., Puechmaille, S. J., & Willis, C. K. (2016) "White-nose syndrome in bats". *Bats in the Anthropocene: Conservation of Bats in a Changing World*. Springer, 245–262.

Hayes, J. P. (1997) Temporal variation in activity in bats and the design of echolocation-monitoring studies. *Journal of Mammology*, **78**.2, 514–524.

Hughes, J. & Haran, M. (2013) Dimension reduction and alleviation of confounding for spatial generalized linear mixed models. *Journal of the Royal Statistical Society: Series B (Statistical Methodology)*, **75**.1, 139–159.

Jiménez-Valverde, A. (2012) Insights into the area under the receiver operating characteristic curve (AUC) as a discrimination measure in species distribution modelling. *Global Ecology and Biogeography*, **21**.4, 498–507.

Johnson, D. S., Conn, P. B., Hooten, M. B., Ray, J. C., & Pond, B. A. (2013) Spatial occupancy models for large data sets. *Ecology*, **94**.4, 801–808.

Kéry, M. & Royle, J. A. (2016) *Applied Hierarchical Modeling in Ecology: Analysis of distribution, abundance and species richness in R and BUGS: Volume 1: Prelude and Static Models*. Academic Press, San Diego, California, USA.

Langwig, K. E., Frick, W. F., Bried, J. T., Hicks, A. C., Kunz, T. H., & Marm Kilpatrick, A. (2012) Sociality, density-dependence and microclimates determine the persistence of populations suffering from a novel fungal disease, white-nose syndrome. *Ecology letters*, **15**.9, 1050–1057.

Langwig, K. E., Frick, W. F., Reynolds, R., Parise, K. L., Drees, K. P., Hoyt, J. R., Cheng, T. L., Kunz, T. H., Foster, J. T., & Kilpatrick, A. M. (2015) Host and pathogen ecology drive the seasonal dynamics of a fungal disease, white-nose syndrome. *Proceedings of the Royal Society B*, **282**.1799, 1–7.

Loeb, S. C., Rodhouse, T. J., Ellison, L. E., Lausen, C. L., Reichard, J. D., Irvine, K. M., Ingersoll, T. E., Coleman, J. T., Thogmartin, W. E., Sauer, J. R., Francis, C. M., Bayless, M. L., Stanley, T. R., & Johnson, D. H. (2015) *A plan for the North American Bat Monitoring Program (NABat)*. General Technical Report SRS-208. Southern Research Station, Asheville, NC: U.S. Department of Agriculture, Forest Service.

MacKenzie, D. I., Nichols, J. D., Lachman, G. B., Droege, S., Andrew Royle, J., & Langtimm, C. A. (2002) Estimating site occupancy rates when detection probabilities are less than one. *Ecology*, **83**.8, 2248–2255.

MacKenzie, D. I. & Royle, J. A. (2005) Designing occupancy studies: general advice and allocating survey effort. *Journal of Applied Ecology*, **42**.6, 1105–1114.

Maxell, B. A. (2015) *Montana bat and white-nose syndrome surveillance plan and protocols 2012-2016*. Tech. rep. Helena, MT: Montana Natural Heritage Program, 205.

Pauli, B. P., Zollner, P. A., & Haulton, G. S. (2017) Nocturnal habitat selection of bats using occupancy models. *Journal of Wildlife Management*, **81**.5, 878–891.

R Core Team (2017) *R: A Language and Environment for Statistical Computing*. R Foundation for Statistical Computing. Vienna, Austria. URL: `https://www.R-project.org/`.

Rodhouse, T. J., Ormsbee, P. C., Irvine, K. M., & Vierlin, L. A. (2012) Assessing the status and trend of bat populations across broad geographic regions with dynamic distribution models. *Ecological Applications*, **22**.4, 1098–1113.

Rodhouse, T. J., Ormsbee, P. C., Irvine, K. M., Vierling, L. A., Szewczak, J. M., & Vierling, K. T. (2015) Establishing conservation baselines with dynamic distribution models for bat populations facing imminent decline. *Diversity and Distributions*, **21**.22, 1401–1413.

Sappington, J. M., Longshore, K. M., & Thompson, D. B. (2007) Quantifying landscape ruggedness for animal habitat analysis: a case study using bighorn sheep in the Mojave Desert. *Journal of Wildlife Management*, **71**.5, 1419–1426.

Severson, R. & Anderson, B. (2016) *countyweather: Compiles Meterological Data for U.S. Counties*. R package version 0.1.0. URL: `https://CRAN.R-project.org/package=countyweather`.

Stan Development Team (2016) *RStan: the R interface to Stan*. Version 2.15.1. URL: `http://mc-stan.org`.

Wibbelt, G., Kurth, A., Hellmann, D., Weishaar, M., Barlow, A., Veith, M., Prüger, J., Görföl, T., Grosche, L., Bontadina, F., et al. (2010) White-nose syndrome fungus (*Geomyces destructans*) in bats, Europe. *Emerging infectious diseases*, **16**.8, 1237–1242.

Wright, W. J., Irvine, K. M., & Rodhouse, T. J. (2016) A goodness-of-fit test for occupancy models with correlated within-season revisits. *Ecology and Evolution*, **6**.15, 5404–5415.

Yackulic, C. B., Chandler, R., Zipkin, E. F., Royle, J. A., Nichols, J. D., Campbell Grant, E. H., & Veran, S. (2013) Presence-only modelling using MAXENT: when can we trust the inferences? *Methods in Ecology and Evolution*, **3**.4, 236–243.

Zipkin, E. F., Campbell Grant, E. H., & Fagan, W. F. (2012) Evaluating the predictive abilities of community occupancy models using AUC while accounting for imperfect detection. *Ecological Applications*, **22**.7, 1962–1972.

Appendix

This Appendix includes additional supporting figures for this report.

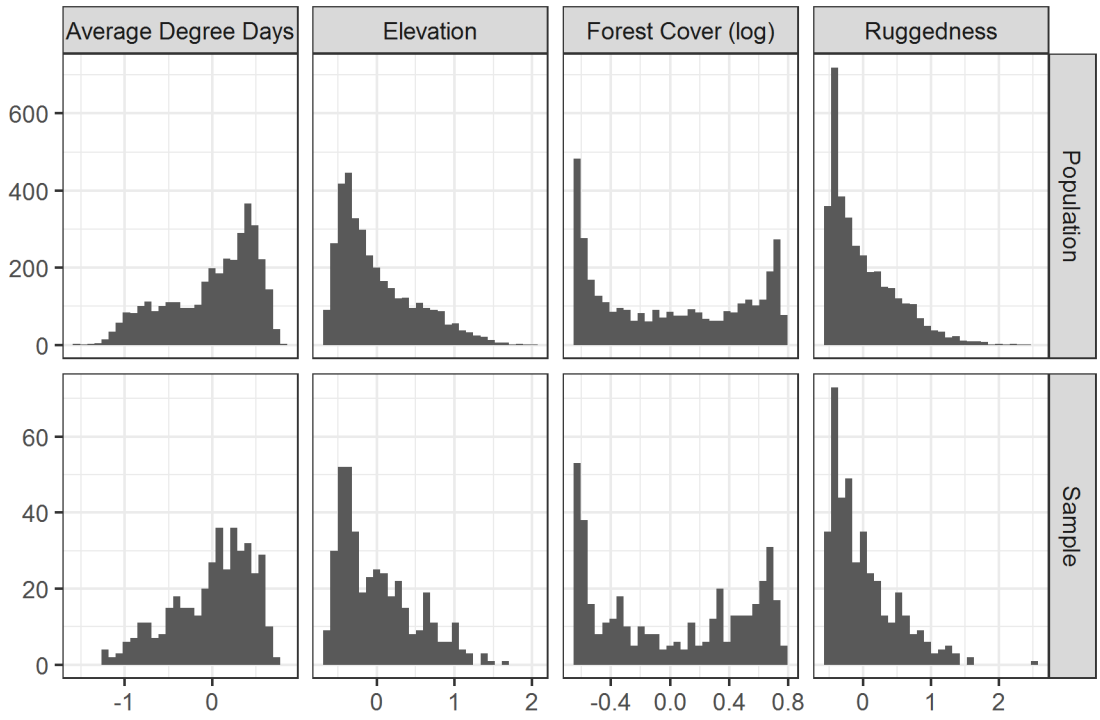

Figure A1: Histograms showing the distributions of the site-level covariates across Montana (population) and within the sampled sites (Sample). For every covariate, the sample appears representative of the population distributions.

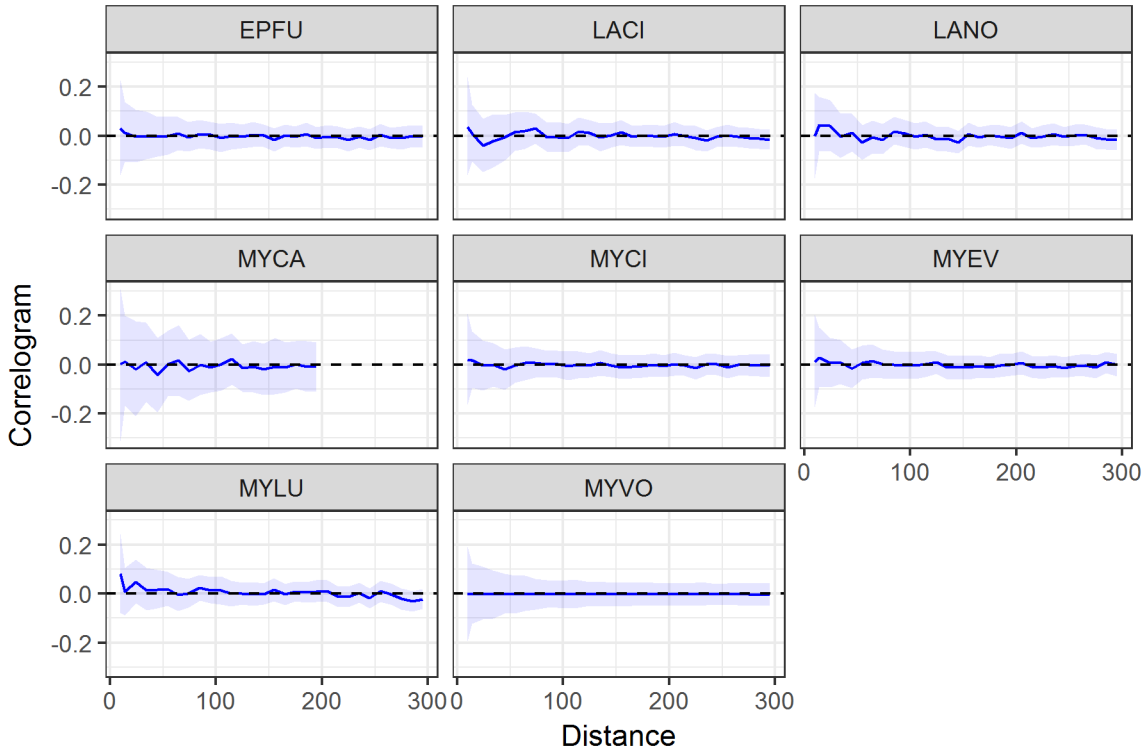

Figure A2: Spatial correlogram of the occupancy residuals based on the initial model which assumed independence for the processes of detection and occupancy. Thick lines show the posterior mean correlation at each distance and the bands show the 95% CI. For each species the bands include zero and provide no evidence of unexplained spatial correlation in the occupancy residuals.

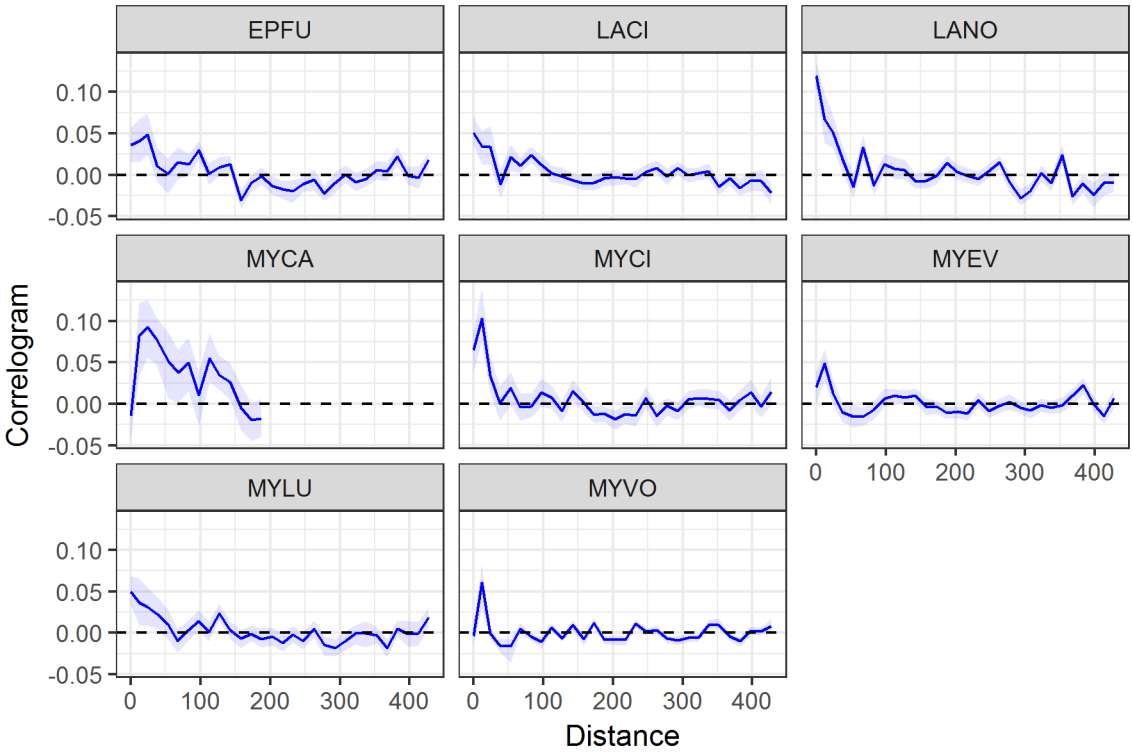

Figure A3: Spatial correlogram of the detection residuals based on the initial model which assumed independence for the processes of detection and occupancy. Thick lines show the posterior mean correlation at each distance and the bands show the 95% CI. Most species show some positive correlation in the residuals at smaller distance classes which provides evidence that detection probabilities are spatially correlated.

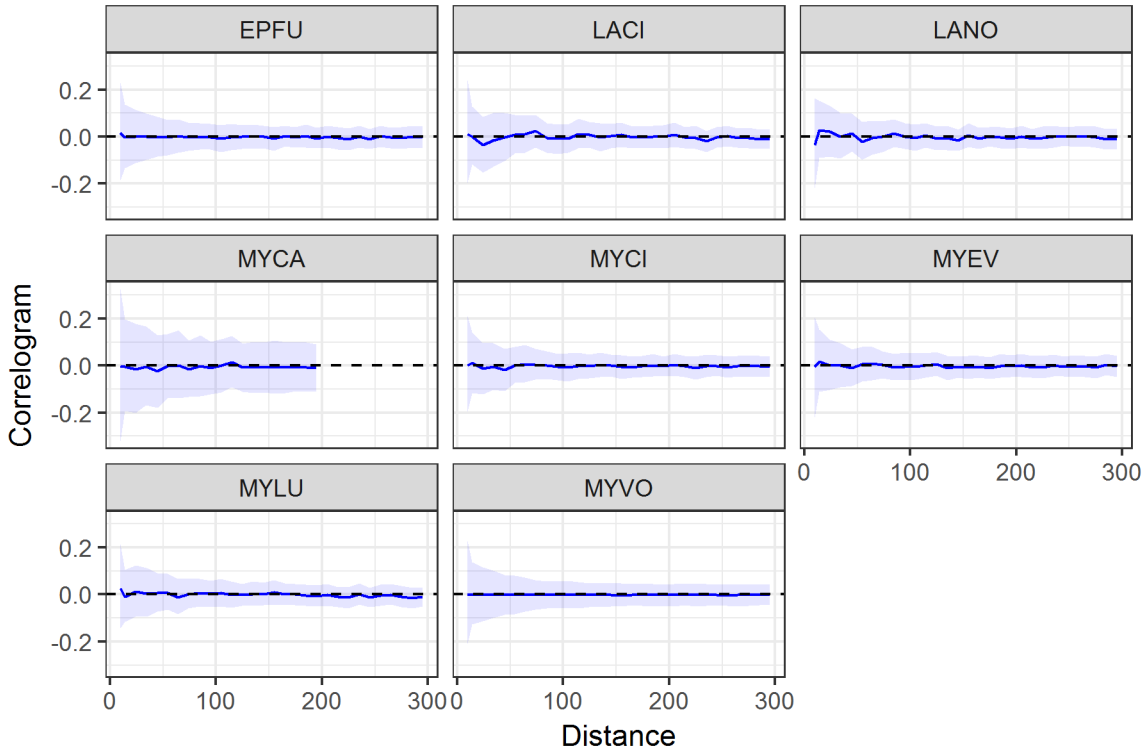

Figure A4: Spatial correlogram of the occupancy residuals from fitting the model which incorporated spatial random effects for detection. Thick lines show the posterior mean correlation at each distance and the bands show the 95% CI. No strong patterns are seen for any species.

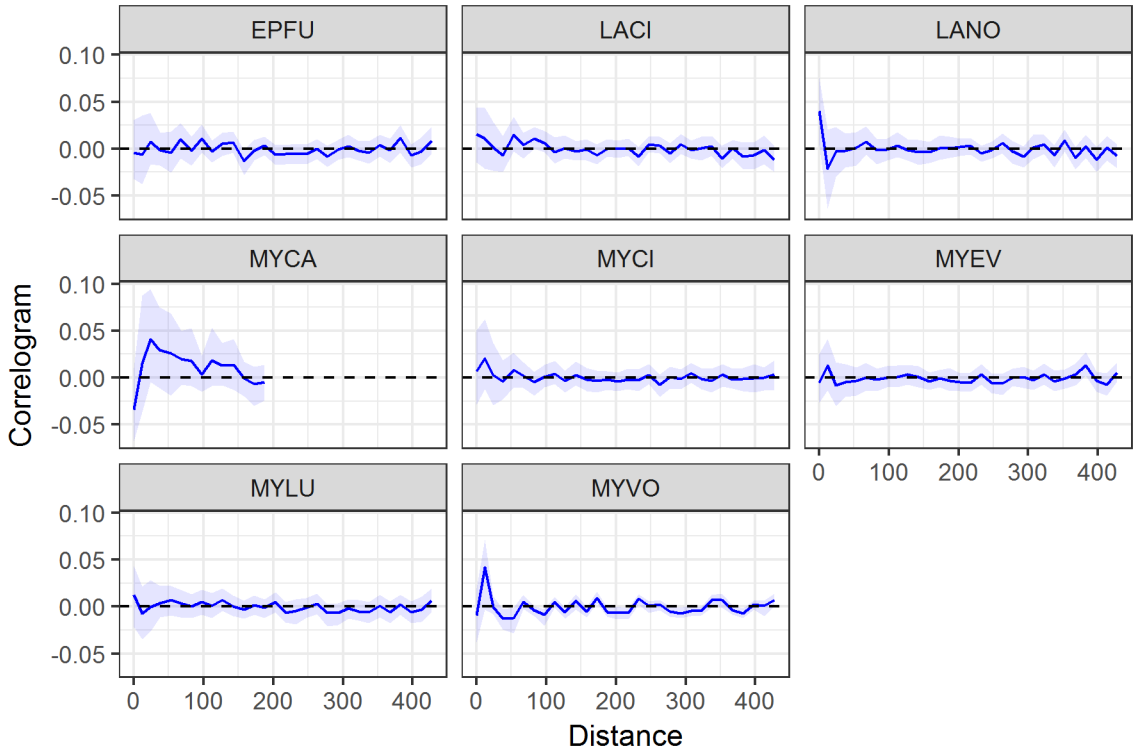

Figure A5: Spatial correlogram of the detection residuals from fitting the model which incorporated spatial random effects for detection. Thick lines show the posterior mean correlation at each distance and the bands show the 95% CI. The patterns in these residuals from the initial model (assuming independence) have been greatly reduced and suggest that including spatial correlation for detection improves the model fit for most species.

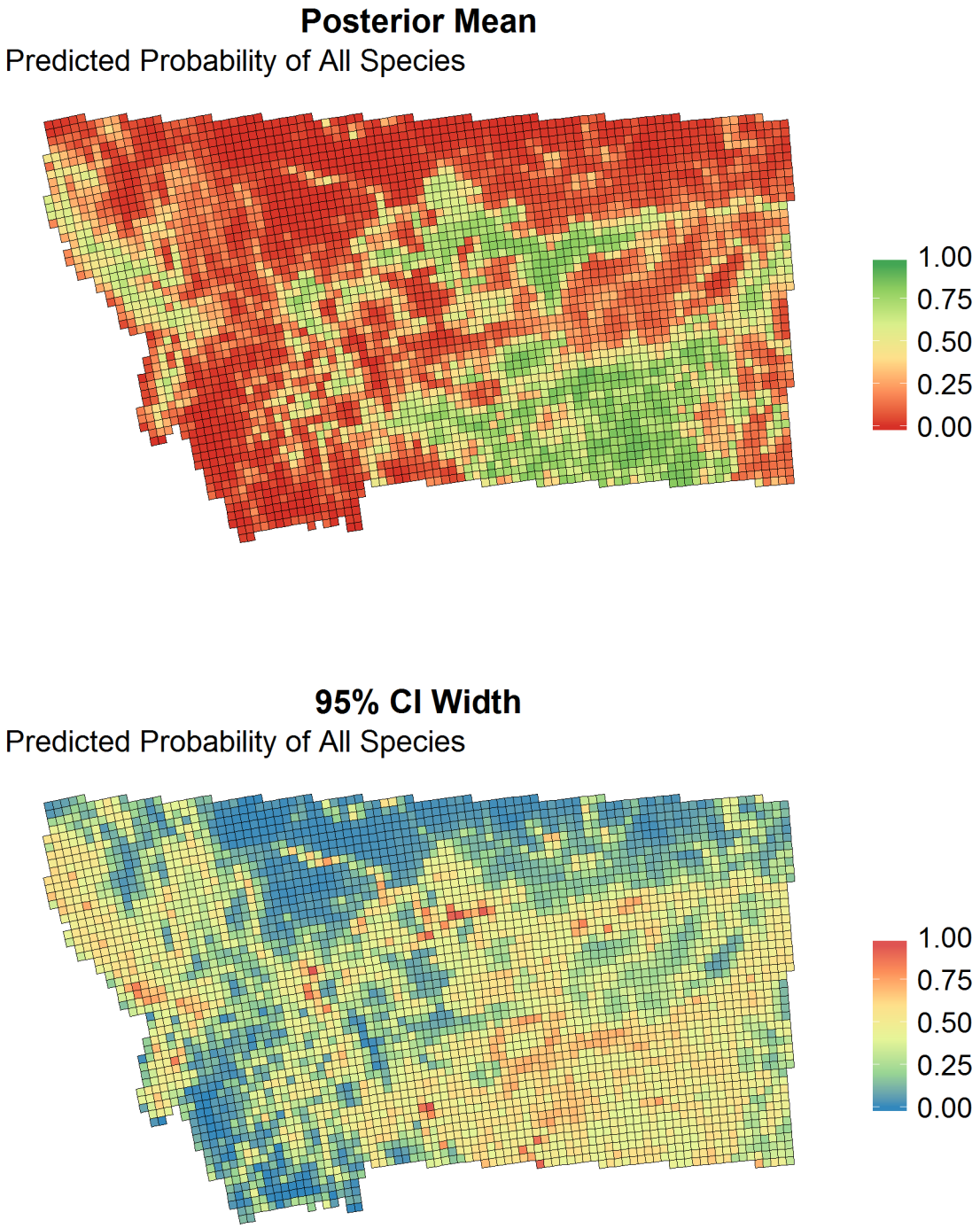

Figure A6: Map of estimated probabilities of joint occupancy for all eight species in this analysis.

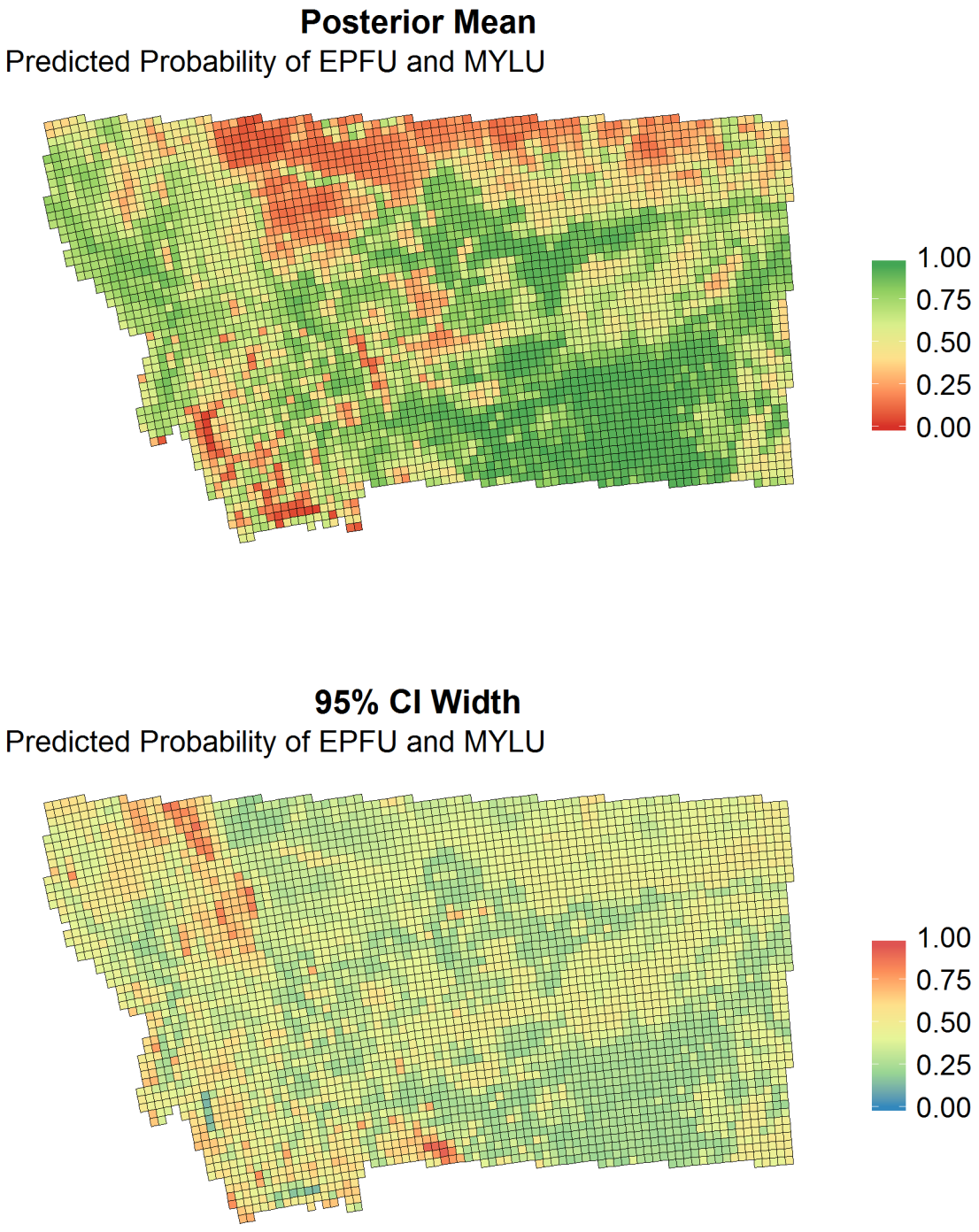

Figure A7: Map of estimated probabilities of joint occupancy for EPFU and MYLU.

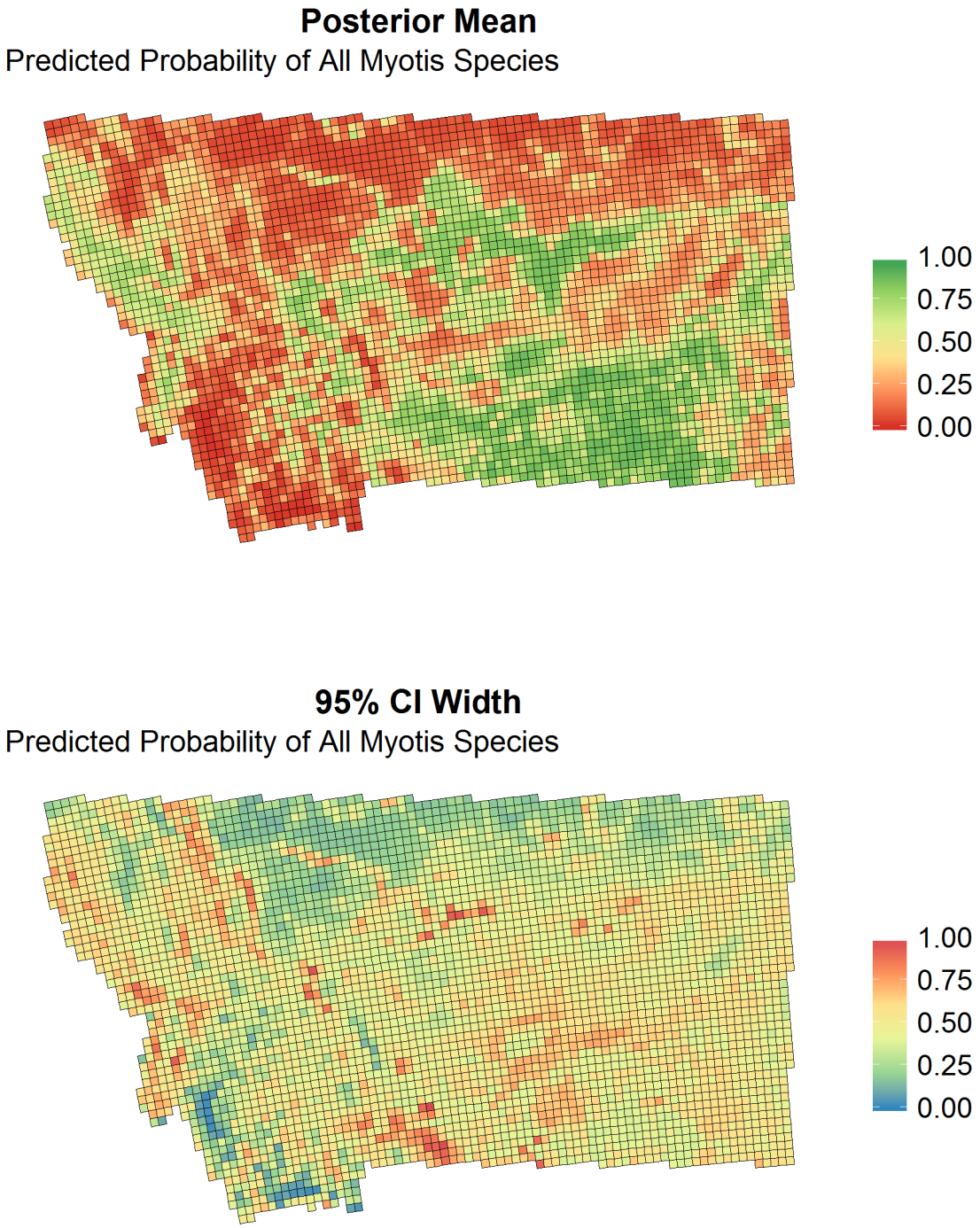

Figure A8: Map of estimated probabilities of joint occupancy for all *Myotis* species in this analysis.

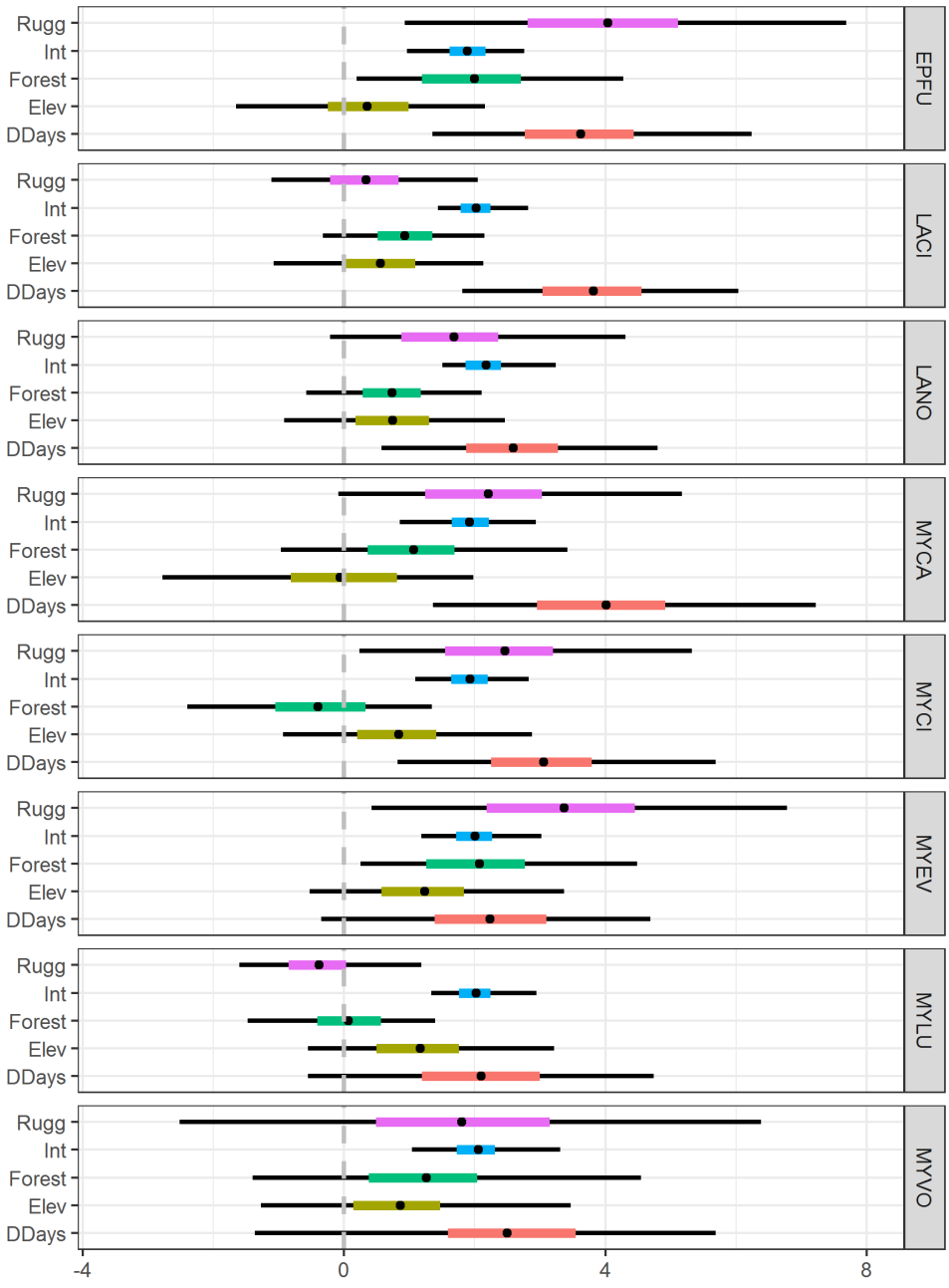

Figure A9: Posterior distributions for the occupancy coefficients of each species. The thinner, black lines show the 95% CIs. The thicker lines show the 50% CIs with the different colors distinguishing the different coefficients. The black points indicate the posterior mean of each parameter.

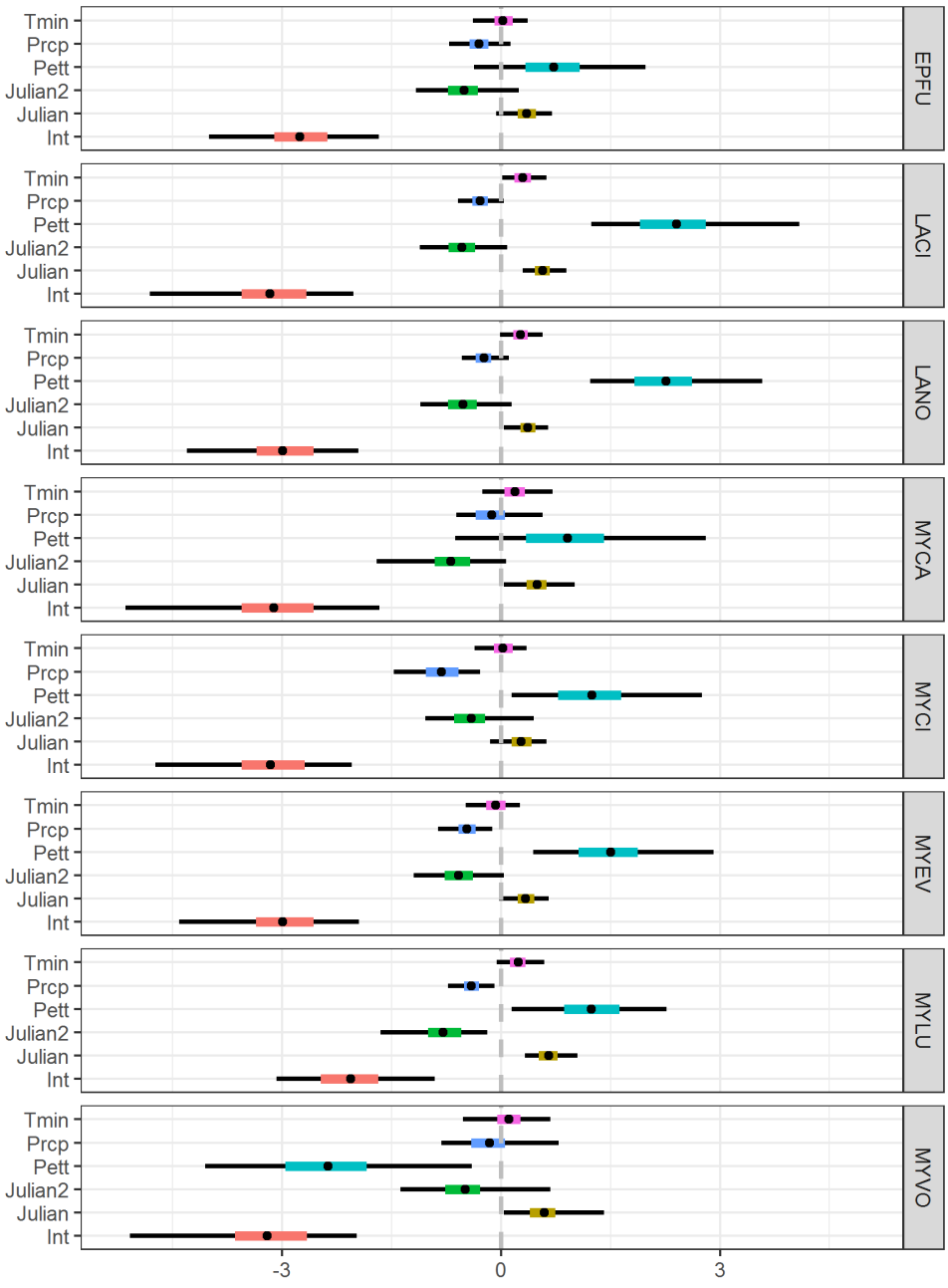

Figure A10: Posterior distributions for the detection coefficients of each species. The thinner, black lines show the 95% CIs. The thicker lines show the 50% CIs with the different colors distinguishing the different coefficients. The black points indicate the posterior mean of each parameter.

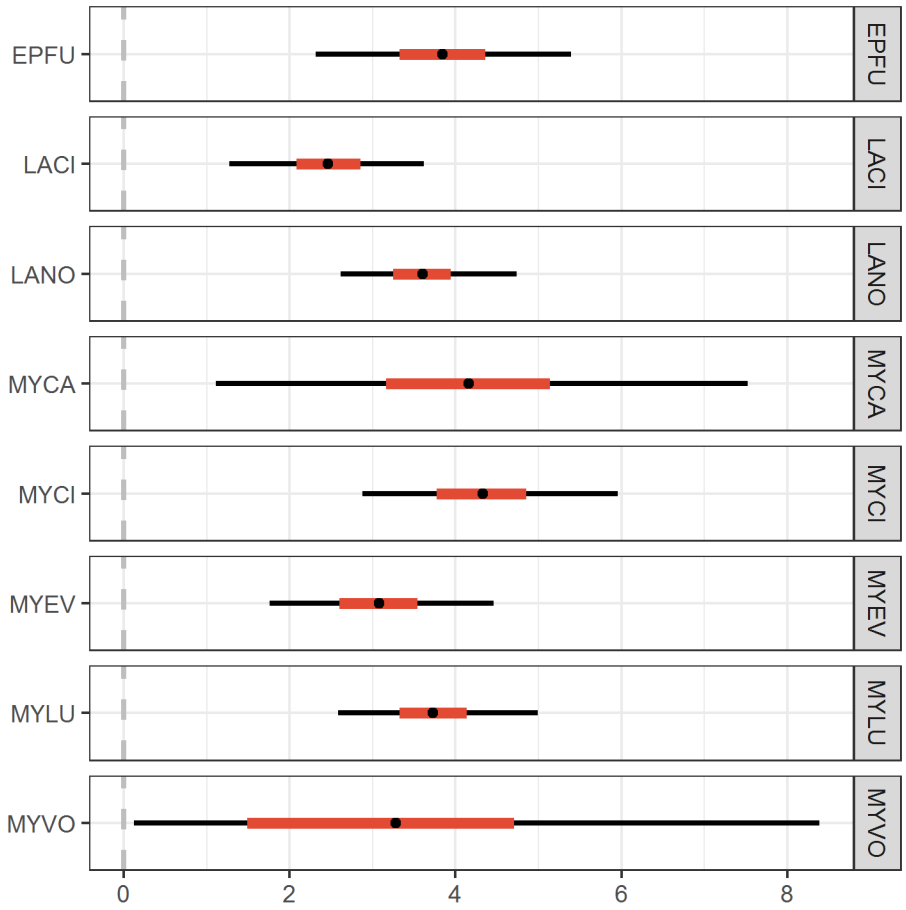

Figure A11: Posterior distributions for the scaling parameters on the spatial random effects for detection probabilities. The 95% and 50% CIs are shown by the black and red lines, respectively. The black dot indicate the posterior means. Except for MYVO, the lower bound of the 95% CIs all appear larger than zero which indicates evidence of spatial correlation in the detection process.

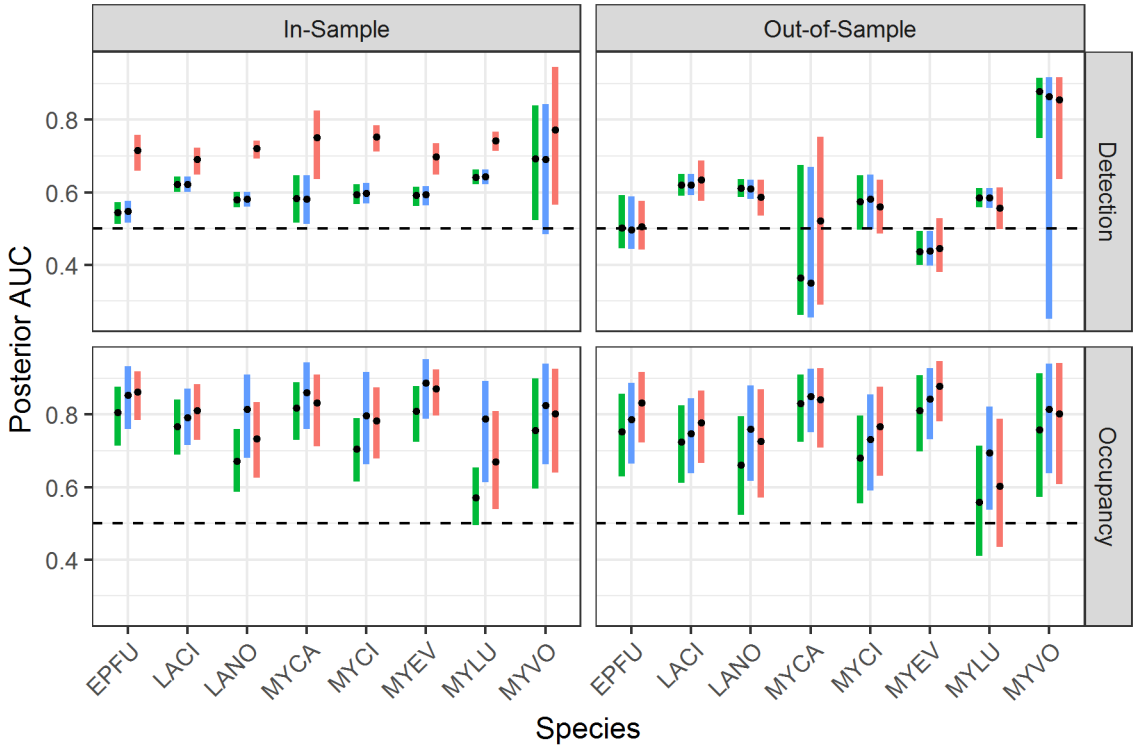

Figure A12: Posterior distributions of the in-sample and out-of-sample AUCs for each species. The AUCs were calculated separately for the occupancy and detection processes. The colors of the line indicate the different models fit with green showing the model assuming independence for both processes, blue for the model with spatial correlation in occupancy probabilities, and red for the model with spatial correlation in detection probabilities. In each case, the lines show the 95% CIs and the black points show the posterior means. There is substantial overlap in most of the AUC posterior distributions across the three models. The most notable exception is for the in-sample detection AUCs where including spatial correlation for detection probabilities appears to improve predictive performance compared to the other two models.